

AD-A072 630

ANALYTICAL METHODS INC BELLEVUE WASH F/G 20/4  
PREDICTION OF AERODYNAMIC CHARACTERISTICS OF FIGHTER WINGS AT H---ETC(U)  
DEC 78 B M RAO, B MASKEW, F A DVORAK N00014-78-C-0128

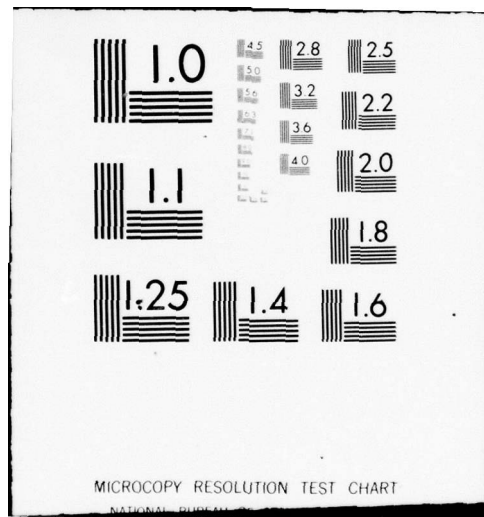
ONR-CR215-258-1

NL

| OF |  
ADA  
072630

END  
DATE  
FILED  
9-79  
DDC

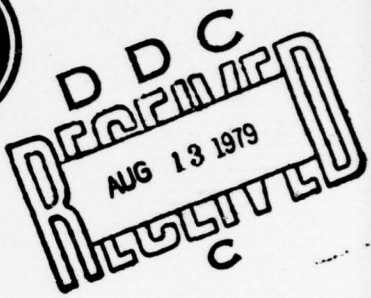
100



■ A 072630



REPORT ONR-CR215-258-1



PREDICTION OF AERODYNAMIC CHARACTERISTICS OF  
FIGHTER WINGS AT HIGH LIFT

BALUSU M. RAO  
BRIAN MASKEW  
FRANK A. DVORAK

ANALYTICAL METHODS, INC.  
100 - 116th AVE. S.E.  
BELLEVUE, WASHINGTON 98004

CONTRACT N00014-78-C-0128  
ONR TASK NR215-258  
31 JULY 1979

INTERIM REPORT FOR THE PERIOD 1 JANUARY - 31 DECEMBER, 1978  
APPROVED FOR PUBLIC RELEASE ; DISTRIBUTION UNLIMITED

DDC FILE COPY



PREPARED FOR THE

OFFICE OF NAVAL RESEARCH • 800 N. QUINCY ST. • ARLINGTON • VA • 22217

79 08 10 016

Change of Address

Organizations receiving reports on the initial distribution list should confirm correct address. This list is located at the end of the report. Any change of address of distribution should be conveyed to the Office of Naval Research, Code 211, Arlington, Virginia 22217.

Disposition

When this report is no longer needed, it may be transmitted to other organizations. Do not return it to the originator or the monitoring office.

Disclaimer

The findings and conclusions contained in this report are not to be construed as an official Department of Defense or Military Department position unless so designated by other official documents.

Reproduction

Reproduction in whole or in part is permitted for any purpose of the United States Government.

UNCLASSIFIED

SECURITY CLASSIFICATION OF THIS PAGE (When Data Entered)

⑨ REPORT DOCUMENTATION PAGE		READ INSTRUCTIONS BEFORE COMPLETING FORM
1. REPORT NUMBER ONR CR215-258-1	2. GOVT ACCESSION NO.	3. RECIPIENT'S CATALOG NUMBER
4. TITLE (and Subtitle) Prediction of Aerodynamic Characteristics of Fighter Wings at High Lift	5. TYPE OF REPORT & PERIOD COVERED Interim 1978 1 January - 31 December	
6. PERFORMING ORG. REPORT NUMBER	7. AUTHOR(s) Balusu M. Rao, Brian Maskew, and Frank A. Dvorak	
8. CONTRACT OR GRANT NUMBER(s) N00014-78-C-0128 fm	9. PERFORMING ORGANIZATION NAME AND ADDRESS Analytical Methods, Inc. 100 - 116th Avenue S.E. Bellevue, Washington 98004	
10. PROGRAM ELEMENT, PROJECT, TASK AREA & WORK UNIT NUMBERS 61153N RR 014-11-84 NR215-258	11. CONTROLLING OFFICE NAME AND ADDRESS Office of Naval Research Code 211, 800 North Quinch Street Arlington, Virginia 22217	
12. REPORT DATE December 31, 1978	13. NUMBER OF PAGES 53	
14. MONITORING AGENCY NAME & ADDRESS (if different from Controlling Office) ⑨ Interim Rept. 1 Jan-31 Dec 78	15. SECURITY CLASS. (of this report) Unclassified	
15a. DECLASSIFICATION/DOWNGRADING SCHEDULE ⑪ 31 Dec 78		
16. DISTRIBUTION STATEMENT (of this Report) Approved for Public Release; Distribution Unlimited ⑫ 57p.		
17. DISTRIBUTION STATEMENT (of the abstract entered in Block 20, if different from Report) ⑯ RR014111 ⑰ RR0141184		
18. SUPPLEMENTARY NOTES		
19. KEY WORDS (Continue on reverse side if necessary and identify by block number) Aerodynamics; separated flows; fighter aircraft; high-lift wings		
20. ABSTRACT (Continue on reverse side if necessary and identify by block number) A basic viscous/potential flow iterative technique is developed for calculating flow on finite wings up to and beyond the stall. The procedure used is a direct adaptation and extension of successfully validated Analytical Methods, Inc. (AMI) two-dimensional CLMAX separation model to three-dimensional flows.		

392 078  
DD FORM 1473 EDITION OF 1 NOV 65 IS OBSOLETE

79 08 10 018 SECURITY CLASSIFICATION OF THIS PAGE (When Data Entered)

Unclassified

SECURITY CLASSIFICATION OF THIS PAGE(When Data Entered)

In the potential flow program, the lifting surface is divided into a number of panels with linear and constant vorticity distributions along the chordwise and spanwise directions, respectively. The separation region is modeled in the potential flow analysis using force-free vortex sheets which require an inner iteration to establish their shapes. The outer iteration loop takes the flow velocity and pressure distributions over to the boundary layer analysis at a selected number of spanwise strips and returns with the separation locations and the boundary layer displacement source distributions. The addition of the source distribution modifies the normal velocity at each control point of the panels. The sources are set to zero in the separated region. The program generates a new wake shape using the new separation locations together with the information from the previous iteration and the process is repeated until a convergent solution is obtained.

In order to expedite the development process, several simplifying assumptions are made. In the separated region, the free vortex sheet deformation is restricted to vertical movements only because of the close-approach problem of the present singularity model which does not permit the full wake roll-up calculation. Additionally, the separation locations, predicted by the boundary layer analysis at each of the selected spanwise stations, are shifted to the trailing edge of the nearest panel on the upper surface of the airfoil. However, these assumptions do not conflict with the primary objective of the present investigation which is to demonstrate the feasibility of extending the two-dimensional CLMAX separation model to three-dimensional flows. The separation flow model and the developed computer program are validated by comparing the results with wind tunnel test data for some simple cases.

Accession For	
NTIS GRA&I	
DDC TAB	
Unannounced	
Justification	
By _____	
Distribution	
Availability Codes	
Dist	Avail and/or special

*(A)*

SECURITY CLASSIFICATION OF THIS PAGE(When Data Entered)

## SUMMARY

A basic viscous/potential flow iterative technique is developed for calculating flow on finite wings up to and beyond the stall. The procedure used is a direct adaptation and extension of the successfully validated Analytical Methods, Inc. (AMI) two-dimensional CLMAX separation model to three-dimensional flows.

In the potential flow program, the lifting surface is divided into a number of panels with linear and constant vorticity distributions along the chordwise and spanwise directions, respectively. The separation region is modeled in the potential flow analysis using force-free vortex sheets which require an inner iteration to establish their shapes. The outer iteration loop takes the flow velocity and pressure distributions over to the boundary layer analysis at a selected number of spanwise strips and returns with the separation locations and the boundary layer displacement source distributions. The addition of the source distribution modifies the normal velocity at each control point of the panels. The sources are set to zero in the separated region. The program generates a new wake shape using the new separation locations together with the information from the previous iteration and the process is repeated until a convergent solution is obtained.

In order to expedite the development process, several simplifying assumptions are made. In the separated region, the free vortex sheet deformation is restricted to vertical movements only because of the close-approach problem of the present singularity model which does not permit the full wake roll-up calculation. Additionally, the separation locations, predicted by the boundary layer analysis at each of the selected spanwise stations, are shifted to the trailing edge of the nearest panel on the upper surface of the airfoil. However, these assumptions do not conflict with the primary objective of the present investigation which is to demonstrate the feasibility of extending the two-dimensional CLMAX separation model to three-dimensional flows. The separation flow model and the developed computer program are validated by comparing the results with wind tunnel test data for some simple cases.

## FOREWORD

The work described in this technical report was performed by Analytical Methods, Inc., for the Department of the Navy, Office of Naval Research, Arlington, Virginia, under Contract Number N00014-78-C-0128. The research program was undertaken under the technical cognizance of Dr. Robert E. Whitehead of the Vehicle Technology Program of ONR.

## TABLE OF CONTENTS

	<u>Page</u>
SUMMARY . . . . .	3
FORWARD . . . . .	4
TABLE OF CONTENTS . . . . .	5
LIST OF FIGURES . . . . .	6
1. INTRODUCTION . . . . .	8
2. BACKGROUND . . . . .	10
2.1 Flow Problem . . . . .	10
2.2 Separated Flow Modelling . . . . .	10
2.3 Close-Approach Technique . . . . .	11
3. DEVELOPMENT OF POTENTIAL FLOW SEPARATION MODEL . . . . .	13
3.1 Modification of the WBAERO Program . . . . .	13
3.2 Separated Wake Region . . . . .	17
3.2.1 Basic Geometry and Paneling of the Wake Sheets . . . . .	17
3.2.2 Wake Sheet Influence Coefficients . . . . .	19
3.2.3 Wake Deformation and Wake Shape Iteration . . . . .	20
4. DEVELOPMENT OF VISCOUS/POTENTIAL FLOW ITERATIVE SCHEME . . . . .	23
4.1 Stagnation Line Flow . . . . .	23
4.2 Boundary Layer Methods . . . . .	24
5. DISCUSSION OF RESULTS . . . . .	27
6. CONCLUSIONS AND FUTURE WORK . . . . .	30
6.1 Conclusions . . . . .	30
6.2 Phase II: Leading-Edge Separation and Close-Approach Model . . . . .	30
7. REFERENCES . . . . .	32

## LIST OF FIGURES

<u>Fig. No.</u>	<u>Title</u>	<u>Page No.</u>
1	Vortex Flows on a Fighter Wing Planform . . . . .	33
2	Simplified Vortex Sheet Model of the Separated Flow . . . . .	34
3	Flow Diagram for the CLMAX Method . . . . .	35
4	Lift and Pitching Moment Characteristics for the GA(W)-1 Airfoil. Reynolds Number = 6.3 Million . . . . .	36
5	Comparison of Calculated and Experimental Pressure Distribution for the GA(W)-1 Airfoil at $20.05^0$ Incidence. Reynolds Number = 6.3 Million . . . . .	37
6	Comparison of Calculated and Experimental Variations of $C_{l_{max}}$ with Reynolds Number for the NACA 4412 Airfoil . . . . .	38
7	Pressures Calculated at Arbitrary Points on a Joukowski Airfoil at $10^0$ Incidence. Model: Submerged Vortices and Sources (Coincident) with Subvortex Technique Applied . . . . .	39
8	Arrangement of the Panels on a Wing . . . . .	40
9 (a)	Chordwise Pressure Distribution ( $y/b = 0.125$ ) .	41
(b)	Chordwise Pressure Distribution ( $y/b = 0.375$ ) .	42
(c)	Chordwise Pressure Distribution ( $y/b = 0.625$ ) .	43
(d)	Chordwise Pressure Distribution ( $y/b = 0.875$ ) .	44
10	Basic Separation Flow Model . . . . .	45
11	Initial Wake Geometry . . . . .	46
12	Chordwise Pressure Distribution (Inboard Section) . . . . .	47
13	Iterated Wake Shapes (Inboard Section) . . . . .	48
14	Chordwise Pressure Distribution ( $y/b = 0.198$ ) .	49
15	Chordwise Pressure Distribution ( $y/b = 0.897$ ) .	50

LIST OF FIGURES (Concluded)

<u>Fig. No.</u>	<u>Title</u>	<u>Page No.</u>
16	Chordwise Pressure Distribution (Strip 1, y/b = 0.18) . . . . .	51
17	Chordwise Pressure Distribution (Strip 3, y/b = 0.695) . . . . .	52
18	Chordwise Pressure Distribution (Strip 5, y/b = 0.95) . . . . .	53

## 1. INTRODUCTION

In the design and analysis of fighter wings, a detailed knowledge of the aerodynamic characteristics at high lift is required, particularly with regard to peak performance in maneuver and during the landing and take-off. The high-lift flowfield is characterized by regions of flow separation both from a conventional trailing-edge type of breakdown and from leading-edge, tip-edge and often part-span separation which lead to vortex lift phenomena giving considerable non-linear effects. In addition, many current designs have vortex flows generated by the forward fuselage or upstream strake which closely interact with the wing. Since attached flow theories are inadequate for those conditions, the aerodynamic characteristics must be obtained from extensive and costly wind tunnel tests. In many cases, however, the wind tunnel tests occur too late in the design cycle to impact the important aerodynamic/structural design trade-offs. The wind tunnel tests, themselves, are not entirely satisfactory because of scale effects. Advanced theoretical methods, therefore, need to be developed that can model the vortex flow and separated flow effects more completely.

Recently, Analytical Methods, Inc. has successfully developed a practical technique for modelling separated flow using free vortex sheets to enclose the low energy region for two-dimensional flows (the details of the method are described in the next section). Under the current contract, this two-dimensional flow model is extended to three-dimensional flows and a basic CLMAX iterative routine involving boundary layer, potential flow and separation modelling is developed. For the potential flow code, an existing program, WBAERO (Wing-Body AERodynamics, developed by Analytical Methods, Inc.), is modified to include the linearly varying vorticity distribution, a convenient singularity model to represent the separated flow regions. For the viscous/potential (outer) iteration schemes, boundary layer

procedure for infinite swept wings is applied using the local information from the potential flow solution at a number of pre-selected spanwise stations. Boundary layer calculations yield the separation points at each of the spanwise stations from which the separated (initial) wake is generated in the potential flow program. The potential flow code also incorporates a wake shape iteration (inner) scheme in which the starting locations of the separation (obtained from the boundary layer solution) at each spanwise station are kept at a fixed position, but the separated wake shapes are iterated until a convergent solution is obtained for each of the outer iterations.

For the current phase of development, the free vortex deformation is restricted to vertical movements only, i.e., no roll-up because of close-approach problems. This is not a serious limitation at this stage, and it has expedited the development of the basic procedure with known models. This restriction will be removed during the next phase of research dealing with the development of a flow model that can handle close-approach problems.

In addition to the trailing-edge separation method, a vortex shedding model is being developed, based on the close-approach techniques, and capable of representing leading-edge separation/vortex formation. In conjunction with this, an edge core model is being developed to "capture" the free vortex sheets as the roll-up calculation proceeds. The reporting of the details of the technique and the results will be delayed until next year when these techniques will be completed and incorporated into the program by using prescribed separation points.

Also, a simple representation of the tip vortex is included in the potential flow model. The results obtained with the present viscous/potential flow iterative scheme are compared with a limited number of available wind tunnel test data and they show good agreement, demonstrating the feasibility of the concept.

## 2. BACKGROUND

### 2.1 Flow Problem

Figure 1 illustrates the nature of the vortex flow at high lift for a fighter wing with leading-edge strakes. To this might be added vortices from the front part of the fuselage and also separated regions from the trailing-edge flow breakdown. Additional flow breakdown will occur during maneuver due to shock/boundary layer interaction, but this is outside the present study. The vortices contribute considerable nonlinear effects which can only be predicted for special cases, e.g., the force--but not the pressure distribution--on sharp-edged delta wings can be predicted (Ref. 1) using potential flow theory and Polhamus' (Ref. 2) suction analogy. Rounded leading-edges and general wing planforms present difficult conditions for theoretical predictions. The complete solution of the viscous/vortex flow using a numerical solution of the Navier Stokes equation is still very remote; however, application of recent developments in analytical methods offers a possible practical procedure in the near future based on boundary layer/potential flow iterative techniques coupled with a free wake analysis. These developments are in the fields of separated flow modelling and in the close iteration between the free separated vortex sheets and the wing. These developments are described briefly in the next two subsections.

### 2.2 Separated Flow Modelling

Recent work (Ref. 3) at Analytical Methods, Inc. has demonstrated an effective, yet practical, technique for modeling separated flow using free vortex sheets to enclose the low energy region (Figure 2). The method combines boundary layer and potential flow codes in an iterative procedure as outlined in Figure 3. An inner iteration is included to determine the shapes of the free vortex sheets. The method has generated accurate  $C_L$  vs.  $\alpha$  curves for several airfoils up to and beyond

the stall at a cost of about \$12 per incidence data point--a mere fraction of the cost of manufacturing and testing a model. The calculation provides the complete pressure distribution, i.e., including that in the separated region at each data point as well as the force and moment values. Comparison between calculated and experimental results are shown in Figures 4 through 6. Lift and pitching moment characteristics with incidence, shown in Figure 4, for the GA(W)-1 airfoil at a Reynolds number of 6.3 million indicate good agreement with experiment up to and beyond the stall. A typical pressure distribution comparison is shown in Figure 5 for the point at  $\alpha = 20.04^\circ$ , i.e., beyond the stall. There is very good agreement even in the separated flow region where the vortex model allows pressures to be calculated directly. Figure 6 shows the good agreement between predicted and experimental variation of  $C_{l_{max}}$  with Reynolds number for the NACA 4412 airfoil.

### 2.3 Close-Approach Technique

One of the major problems of predicting the vortex/surface non-linear interaction using panel methods is the "close-approach" situation. Panel methods have distortions in the velocity distribution close to the panel edges, and these give rise to divergent behavior when calculating the trajectory of vortex lines in free wake analysis. The problem is present in varying degrees of severity in all panel methods including the recent higher-order methods. The problem was investigated for vortex singularities in two-dimensional flow, and a subvortex technique developed (Ref. 4) which demonstrates negligible flow distortion along the surface. For example, Figure 7 shows the pressure distribution calculated directly at arbitrary points (i.e., not related to the singularity positions) on the surface of a Joukowski airfoil. Without the close-approach technique, these pressure values would have a wildly oscillating distribution.

This close-approach technique is now being extended to the three-dimensional case under NASA funding. In this

extension, it has been found more convenient to represent the vortex sheets with doublet singularities. These are coupled with source singularities using the symmetrical singularity principle (Ref. 5) developed at Analytical Methods, Inc. This principle minimizes the singularity strengths and thereby reduces errors associated with the singularity modelling.

### 3. DEVELOPMENT OF POTENTIAL FLOW SEPARATION MODEL

The current phase of this study primarily deals with trailing-edge separations, since this is less dependent on the availability of the close-approach model described in Section 2. In this study, the basic viscous/potential flow/wake iterative procedure in the two-dimensional CLMAX method is extended to the three-dimensional case. In this section the development work on the modification of an existing potential flow code, incorporation of the separation model, and wake shape iteration (inner) schemes are described. Some results are presented validating the developed model.

#### 3.1 Modification of the WBAERO Program

WBAERO is a wing-body aerodynamics program in which a lifting surface is divided into a number of panels, each of which contains a constant source distribution and an internal vortex lattice. Analytical expressions for the velocity induced by a constant source distribution and also by the elements of a vortex-lattice are used to calculate the coefficients of a system of linear equations relating the magnitude of the normal velocities at the panel control points to the unknown source and vortex strengths. The source and vortex strengths which satisfy the boundary condition of tangential flow at the control points for a given flow condition are determined by solving the system of equations by an iterative procedure.

In the present program, the constant source panels in WBAERO are replaced by vorticity panels, assuming a linear and a constant distribution along the panel chord and the span, respectively. The equations are set up to solve for vorticity distribution. The source panels are still there, but take on values derived from the boundary layer displacement, the details of which are explained in the next section. For the attached flow case, the procedure is very similar to the existing code.

The lifting surface is divided into a number of chordwise and spanwise panels, over each of which the vorticity is assumed to

vary linearly from the leading to the trailing edge. Assuming that there are  $N$  chordwise panels at a given spanwise station, there are  $N+1$  unknowns,  $\gamma_1, \gamma_2, \dots, \gamma_{N+1}$ , where  $\gamma_1$  and  $\gamma_{N+1}$  are vorticity strengths at the leading edge of the lower surface panel (panel 1) and the trailing edge of the upper surface (panel  $N$ ), respectively. However, the application of a Kutta condition at the trailing edge of an airfoil yields  $\gamma_1 = \gamma_{N+1} = 0$ , resulting in  $N-1$  unknowns but  $N$  linear equations. An unknown uniform source distribution is assumed over the airfoil surface at each spanwise station resulting in a consistent set of linear equations.

The velocity induced at any panel,  $i$ , due to the linearly varying vorticity distribution at another panel,  $k$ , can be expressed as a sum of several components (see Figure 8):

$$\begin{aligned}
 v_{ik} = & \text{ADCV}_{ik} \gamma_k + \text{ADLV}_{ik} (\gamma_{k+1} - \gamma_k) \\
 & + \text{ACV}_{ik} \left[ \left( \gamma_{ks} s_{ks} + \gamma_k s_{k-1} \right) \right] / 2 \\
 & + \sum_{\ell=ks+1}^{k-1} \gamma_{\ell} \left( s_{\ell} + s_{\ell-1} \right) / 2
 \end{aligned} \tag{1}$$

where

$v_{ik}$  velocity induced at the  $i^{\text{th}}$  panel due to linearly varying distributed vorticity ( $\gamma_k$  to  $\gamma_{k+1}$ ) at panel  $k$   
 $\text{ADCV}_{ik}$  velocity induced at  $i^{\text{th}}$  panel due to a unit constant distributed vorticity at panel  $k$

$ADLV_{ik}$  velocity induced at  $i^{\text{th}}$  panel due to a unit linear distributed vorticity at panel  $k$

$ACV_{ik}$  velocity induced at  $i^{\text{th}}$  panel due to a unit constant vortex at panel  $k$

$ks$  the first chordwise panel at the spanwise station of  $k^{\text{th}}$  panel ( $= k - n+1$ )

$\gamma_k$  the distributed vorticity strength at the start of panel  $k$

Note that the summation multiplier of  $ACV_{ik}$  represents the cumulative distributed vorticity up to panel  $k$  at that spanwise station.

The various influence coefficients,  $ADCV$ ,  $ALDV$ ,  $ACV$ , for all the panels are computed as three component vectors representing the three components of the velocities along the  $x$ ,  $y$ , and  $z$  axes, respectively. The Influence Coefficient Matrix,  $[AM]$ , consists of the normal velocity components, and is expressed as

$$\{V_N\} = [AM]\{\gamma\} \quad (2)$$

where  $\{V_N\}$  is the normal velocity vector at the panels on the wing surface. The Influence Coefficient Matrix is assembled by using Eqn. (1), and the surface normal vectors at the panels. The three component velocity vectors ( $VX$ ,  $VY$ , and  $VZ$ ) are also stored and used to find the velocity, and hence the pressure distributions on the wing surface, once the  $\gamma$  distribution is obtained by solving Eqn. (2)

The modified potential flow code is checked out on a simple case of rectangular wing of aspect ratio 2 with an 11.17% thick TR17 airfoil section (Boeing wing). This particular wing has been extensively used as a test case for evaluating several panel methods and the data is available for comparison. The wing is divided into 144 panels (36 chordwise and 4 spanwise) and the angle of attack is  $5.73^\circ$ . The computed results are compared with those of USSAERO (a symmetric singularity method) and the Doublet Code (close-approach doublet model). The Doublet Code has been developed by AMI under a NASA contract and it will be replacing the present potential flow code during the next phase of the current research. In the doublet code, a semi-circular tip representation is included in addition to the four spanwise strips. The comparison for the lift coefficients is given below.

<u>Section Lift Coefficients</u>			
$y/b$	PRESENT	USSAERO	DOUBLET
0.125	0.3141	0.3264	0.3375
0.375	0.2981	0.3092	0.3204
0.625	0.2635	0.2694	0.2781
0.875	0.2078	0.1920	0.1712
$c_L$	0.2762	0.2740	0.2768

The pressure distribution at the four spanwise stations are shown in Figures 9(a) through 9(d). As can be seen from these figures, the pressure distribution comparison looks good except at the tip section ( $y/b = 0.875$ ), which can be attributed to the fact that in the present model in computing the pressure distribution, the surface velocity induced by the spanwise variation of vorticity is not taken into account. This will be corrected in the next phase of research when the close-approach potential flow model is incorporated.

### 3.2 Separated Wake Region

The current phase of research deals with the trailing-edge separation only and hence the separation is limited to the region extending from the separation line to the trailing edge over the upper surface of the wing. The arbitrary separation line is computed from the boundary layer solutions starting from a potential flow solution (viscous/potential flow iteration) at a preselected number of spanwise stations. The details of the viscous/potential flow (outer) iterative scheme are presented in the next section. The present singularity model of linearly varying chordwise and constant spanwise vorticity panels restricts the free vortex deformation to vertical movements only; i.e., no roll-up because of close-approach problems. Additionally, the arbitrary separation line is modified in such a way it is discontinuous and is shifted parallel to the trailing-edge of the nearest panel at each of the selected spanwise sections (see Figure 10). These simplifying assumptions are made to expedite the development of the program to demonstrate the feasibility of the separation model for three-dimensional flows, and these restrictions will be removed during the next phase of the development.

#### 3.2.1 Basic Geometry and Paneling of the Wake Sheets

Starting from an initial potential (attached) flow solution, the boundary layer analysis predicts the separation locations at each of the selected spanwise sections providing the locus of the arbitrary separation line. As explained earlier, for the current phase these separation locations are modified in such a way that they are shifted parallel to the trailing edges of the nearest panels in the separation region. Initially, the separated streamlines are not known, and so the shapes of the free shear layers must be obtained iteratively starting from an initial assumption. For the current phase, the streamlines are assumed to lie in vertical streamwise planes, and hence can be completely described by two coordinates (x and z) only at any spanwise (y)

cross section. The initial wake geometry adopted at any spanwise section is shown in Figure 11. This initial wake geometry proved to be adequate for the two-dimensional separated flow program; however, the number of wake iterations can be reduced substantially by a proper choice of the slope of the intial wake over the upper surface. The upper and lower separated wake sheets (panels) are represented by parabolic curves passing from the separation points to a common point downstream. The slope at the upstream end is the mean between the free stream direction and the local surface slope. The common point downstream is positioned on the mean wake line, distance  $WL$  downstream from the wake mid-point. Several ways of defining the wake length,  $WL$ , were investigated during the development of the two-dimensional CLMAX program for a number of different airfoils. The best model was based on a "fineness ratio" of the wake; i.e.,  $WL$  is obtained by multiplying the "height" of the wake by the wake "fineness ratio",  $WF$ , which is a function of the airfoil shape. This model is adopted in the present program.

The adopted separation model assumes that the vorticity over the upper and lower surface wake panels at any spanwise strip is a constant equal in magnitude to the vorticity strength at the separation line (the trailing edge of the panel at which separation occurs). A convenient (adequate) number of uniform vorticity panels are constructed along the curves in the wake separation region over the upper surface up to a common line downstream in such a way that the panel edge points correspond approximately with those on the surface below so that interference velocities can be reliably calculated if the wake sheet lies close to the surface. Similar types of uniform vorticity (strength is equal and opposite to the strength of the separation vortex sheet over the upper surface) panels are constructed along the curves from the lower surface trailing edges to the common line intersecting the wake separation region over the upper surface. The geometry of the panels in the separation region and their

normal and tangent vectors are computed using the same subroutines used to compute the surface panel information.

### 3.2.2 Wake Sheet Influence Coefficients

Since the uniform vorticity in the separation region can be expressed as a function of the vorticity strengths at one or more panels on the surface that are affected by the separation, the process does not introduce any additional unknown vorticity strengths. For the present program, since the separation line at any spanwise section is assumed to coincide with the trailing edge of a panel, the vorticity strength in the separation region is equal to the trailing vorticity strength at the separation panel, which is one of the computed unknowns in the solution matrix. Hence, the size of the Influence Coefficient Matrix is not affected by the presence of the separation regions. The three components of the velocity vector induced by the panels in the separation region (assuming uniform vorticity of unit strength) are computed for all of the surface panels on the wing, and are stored in appropriate velocity component arrays, making use of the relation that the separated vortex sheet strength is equal to the vorticity strength at the trailing edge of the separation panel. From these velocity component arrays, the Influence Coefficient Matrix (the elements of which are the normal components of the velocities induced at any surface panel due to another panel) are computed and stored on tape. Also, the velocity components induced at the panel edges in the separation region due to the surface and the wake panels are computed and stored on tape which is used later in the Wake Deformation and Wake Shape Iteration calculation to arrive at the new wake (iterated) geometry after each iteration and also for computing the pressure distribution in the wake region.

### 3.2.3 Wake Deformation and Wake Shape Iteration

Once the influence coefficient matrix is generated for the initial wake, the separated flow solution can be obtained yielding the vorticity distribution over the airfoil surface and the separated wake sheets. From this known vorticity distribution, the velocity components on the upper and lower wake panels can be computed and from these the new wake shape is generated. At the present time, only the x and z components of the velocity are taken into account, neglecting the lateral (spanwise) motion of the wake sheets. The upper and lower separated wake sheets, which are joined to a common line downstream for the initial wake, are permitted to terminate at two separate lines. This results in a physically inconsistent situation since the two wake sheets with finite vorticity are permitted to terminate abruptly. However, this may be justified as a reasonable approximation based on the previous experience with the two-dimensional CLMAX program. The deformed wake panel coordinates are computed and the new influence coefficient matrix is generated. The flow solution using the deformed wake is obtained and the process is repeated using the iterated wake.

The development of the wake iteration scheme is checked out on a simple case of a rectangular wing of aspect ratio 6 and an angle of attack of  $12^{\circ}$ . The semi-wing is divided into 114 panels (38 chordwise and 3 spanwise strips) and the separated wake sheets over the three spanwise strips are divided into 36 segments. For the representation of the separated flow, the flow is assumed to separate at  $x/c = 0.5, 0.7$  and  $0.8$  over the upper surface (arbitrary just for the purpose of checking the separation model and the wake iteration scheme; in the final program, the separation locations are obtained from the boundary layer solutions) at the inboard, center and outboard sections, respectively.

The computed local lift coefficients for the attached flow, initial wake, and first wake iteration are given below.

<u>Section</u>	<u>Attached Flow</u>	<u>Initial Wake</u>	<u>First Wake Iteration</u>
Inboard	0.9982	0.2463	0.3122
Center	0.9715	0.7976	0.8323
Outboard	0.7734	0.6675	0.7013

The pressure distribution and the iterated wake shapes for the inboard section are presented in Figures 12 and 13, respectively. As may be seen from these figures, the wake iteration scheme may be completely avoided if a proper guess can be made for the initial wake. The most important factor in the description of the initial wake is the slope at the separation location on the upper surface which is a strong function of angle of attack.

TABLE I. RECTANGULAR WING,  $\alpha = 19.56^\circ$ 

CHORDWISE STATION	VORTICITY STRENGTHS ( $\gamma/4\pi$ )		
<u>Number &amp; Location (x/c)</u>	<u>Strip 1</u>	<u>Strip 2</u>	<u>Strip 3</u>
1. 1.000	-.0792	-.0740	-.0577
2. 0.995	-.0710	-.0652	-.0479
3. 0.980	-.0670	-.0615	-.0511
4. 0.955	-.0727	-.0687	-.0433
5. 0.921	-.0735	-.0708	-.0431
6. 0.878	-.0630	-.0636	-.0481
7. 0.827	-.0571	-.0602	-.0527
8. 0.770	-.0569	-.0603	-.0561
9. 0.708	-.0578	-.0610	-.0584
10. 0.641	-.0584	-.0614	-.0600
11. 0.571	-.0585	-.0613	-.0611
12. 0.500	-.0579	-.0607	-.0617
13. 0.429	-.0565	-.0594	-.0617
14. 0.359	-.0542	-.0572	-.0611
15. 0.292	-.0508	-.0539	-.0596
16. 0.230	-.0456	-.0490	-.0566
17. 0.173	-.0384	-.0422	-.0515
18. 0.122	-.0278	-.0321	-.0435
19. 0.079	-.0118	-.0169	-.0309
20. 0.045	.0141	.0076	-.0105
21. 0.020	.0597	.0510	.0267
22. 0.005	.1502	.1347	.1011
23. 0.000	.2683	.2520	.2057
24. 0.005	.2735	.2608	.2224
25. 0.020	.2180	.2121	.1838
26. 0.045	.1842	.1791	.1585
27. 0.079	.1615	.1576	.1410
28. 0.122	.1456	.1423	.1281
29. 0.173	.1333	.1307	.1178
30. 0.230	.1233	.1212	.1092
31. 0.292	.1147	.1131	.1016
32. 0.359	.1073	.1060	.0948
33. 0.429	.1002	.0996	.0887
34. 0.500	.0936	.0936	.0832
35. 0.571	.0873	.0878	.0781
36. 0.641	.0810	.0822	.0732
37. 0.708	.0744	.0765	.0683
38. 0.770	.0675	.0707	.0629
39. 0.827	.0593	.0645	.0567
40. 0.878	.0689	.0673	.0492
41. 0.921	.0792	.0740	.0396
42. 0.955	.0007	.0014	.0439
43. 0.980	-.0004	-.0004	.0577
44. 0.995	-.0004	-.0004	-.0003
45. 1.000	0	0	0

Separation Region

#### 4.0 DEVELOPMENT OF VISCOUS/POTENTIAL FLOW ITERATIVE SCHEME

The boundary layer development on an arbitrarily-shaped lifting configuration with separated flow is very complex. A thorough and exact calculation of this development is properly the domain of the time-dependent solution to the general Navier Stokes equations. Unfortunately the computer does not yet exist which is capable of handling such a problem in a cost-effective manner. Less difficult or costly are the finite-difference boundary layer programs now in existence. The amount of computer time for each calculation still prohibits their use in an analysis type procedure. Having made the above evaluation, one must conclude that if the objective is a viscosity-dependent calculation procedure of practical use to the aerodynamicist for analysis at high angles of attack, and possibly for preliminary design, the method must be relatively simple to use and be cost effective. This can be achieved if integral boundary layer methods are used. It is anticipated that integral methods will be adequate for most applications of practical interest to the aerodynamicist for flow calculations at high angles of attack in the attached flow region. Hence the integral boundary layer methods are adopted in the current program.

The finite span wing is divided into a number of streamwise strips. Each strip is treated as if it were a separate infinite swept wing. On each strip the boundary layer development is calculated along streamlines from the stagnation line to the trailing edge of each element using the integral boundary layer methods.

##### 4.1 Stagnation Line Flow

Theoretical prediction of the stagnation line flow of an infinite yawed wing by Cumpsty and Head (Ref. 6) and Bradshaw (Ref. 7) as well as others indicates that the boundary layer approaches an asymptotic state where frictional forces are balanced by divergence of the flow from the spanwise to the streamwise direction. Cumpsty and Head found that the stagnation line boundary layer integral parameters ( $H$ ,  $\theta$ , and  $C_f$ ) and the

state (laminar or turbulent) correlate with the parameter,  $C^* = V^2/(2du/ds)$ . Cumpsty and Head (Ref. 8) later experimentally verified their theoretical correlations, and it is these correlations that are used to determine the boundary layer characteristics on each element of the swept finite wing. If the wing is unswept, then conventional two-dimensional correlations are used to start the boundary layer calculations.

#### 4.2 Boundary Layer Methods

If the Reynolds number is sufficiently low to allow laminar flow on a swept wing, the two-dimensional equations of Curle (Ref. 9) are solved along external streamlines to determine the laminar boundary layer development. It is assumed that the laminar cross-flow effects have a negligible influence on the overall calculation, at least for moderate sweep angles.

The streamwise boundary layer characteristics are used with the correlation of Smith (Ref. 10) to determine the point of laminar instability. With the point of instability, the momentum thickness Reynolds number distortion,  $R_\theta$ , and the pressure gradient parameter,  $\bar{k}$ , known, the transition point is determined using Granville's correlation (Ref. 11). The turbulent boundary layer development over an infinite swept wing is calculated using the method of Cumpsty and Head (Ref. 12). If the initial stagnation line flow is turbulent, Cumpsty and Head's method is used from the stagnation line to the element trailing-edge.

In those cases where laminar separation occurs prior to transition, a correlation band on the data of Gaster (Ref. 13) is used to determine if turbulent reattachment occurs. Should reattachment be predicted, the calculation continues for turbulent flow; if catastrophic separation is predicted, the boundary layer calculation is terminated.

The boundary layer solution predicts the separation location over the upper surface and the source strength distributions to represent the boundary layer displacement thickness over the airfoil surface at each of the selected spanwise strips. This information is passed back to the potential flow program to start the next iteration. The separation (initial) wake is generated according to the separation points computed at the selected strips adopting the procedure explained in the previous section and the wake is iterated until a convergent solution is obtained. It is assumed that the source distributions representing the boundary layer displacement thickness in the attached flow region affect only the normal boundary condition on the surface, and hence the right-hand side of the solution matrix. Also, the effect of the source distributions in the separation region is neglected.

The viscous/potential flow iterative scheme is checked out on a simple case of a rectangular wing of aspect ratio 6 (NASA Langley wing--NACA 0012 section) at an angle of attack of  $19.56^{\circ}$ . The primary reason for selecting this wing is the availability of an extensive set of wind tunnel test data covering a wide range of angles of attack and sweep angles. The semi-wing is divided into 132 panels (44 chordwise and 3 spanwise strips) and the separated wake sheets over the three spanwise strips are divided into 36 segments. The computed local lift coefficients for the attached and separated flows (after one viscous/potential flow iteration with initial wake) and the locations of the separation points predicted by the boundary layer solution are given below.

SECTION (% semi-span)	$C_l$ Potential Flow	Separated Flow	SEPARATION LOCATION (% local chord)
19.8	1.566	1.368	90.2
44.8	1.436	1.278	91.8
89.7	1.024	0.931	97.4

The pressure distributions at the inboard and outboard sections are presented in Figures 14 and 15, respectively.

In the accompanying table, the vorticity distribution computed for the separated flow is given. The chordwise station numbers start at the lower surface trailing-edge (1) and continue along the airfoil in a counterclockwise direction towards the upper surface trailing edge (45). As expected, the vorticity values in the separation region are low, and the boundary condition that the vorticity (uniform) over the upper surface wake sheet is equal in magnitude and opposite in sign to the vorticity over the lower surface wake sheet is satisfied. The results indicate that the program is working and we can conclude that the adopted separation model is reasonable at this stage.

## 5. DISCUSSION OF RESULTS

In addition to the development of the program described in Sections 3 and 4, a simple tip vortex model is incorporated into the program. The tip vortex model assumes that at the last spanwise strip (near the tip), the flow separates from the upper surface in the region from the maximum thickness location to the trailing edge at an inclination angle which is a function of the angle of attack ( $\alpha$ ). Usually the inclination is assumed to be  $0.5\alpha$  or less, depending on the value of  $\alpha$ . The program has the option of either including or excluding the tip vortex.

The method was applied to an Aspect Ratio 6 constant chord wing (NASA Langley wing--NACA 0012 section). An extensive set of wind tunnel test data is available for this wing covering a wide range of angles of attack and sweep angles. The semi-wing is divided into 220 panels (44 chordwise x 5 spanwise) and the selected spanwise locations are given below.

<u>Station No.</u>	<u>Fraction of Semi-Span (y/b)</u>
1	0.180
2	0.485
3	0.695
4	0.840
5	0.950

The results at low angles of attack are not included in this section since they were already presented in Section 3, validating the potential flow program. The computed and experimental chordwise pressure distributions for the case of  $\alpha = 19.56^\circ$  and sweep angle of  $0^\circ$ , are shown in Figures 16, 17, and 18 at the spanwise strips 1, 3, and 5, respectively. For the computation, a total of three viscous/potential flow iterations with no wake iterations (i.e., with initial wake only). As can be seen from these figures, the inclusion of the tip vortex model does

not have any significant effect on the pressure distribution except at the tip section and the results compare well with the experiment (wind tunnel test).

The next set of computed results were for the case of a wing with the sweep angle of  $9.72^\circ$  at  $\alpha = 21.38^\circ$ . A total of six viscous/potential flow iterations were performed and the results of local lift coefficients and the separation locations for the six iterations are tabulated in the following tables.

STRIP NO.	SECTION LIFT COEFFICIENTS					
	ITERATION NO.					
1 (Pot. Flow)	2	3	4	5	6	
1	1.625	1.289	1.153	1.154	1.078	1.080
2	1.563	1.000	1.053	1.045	1.037	1.037
3	1.415	1.154	1.038	1.050	1.050	1.048
4	1.181	1.003	0.986	0.912	0.929	0.931
5	1.839	0.752	0.739	0.742	0.726	0.777

STRIP NO.	UPPER SURFACE SEPARATION LOCATIONS (X/C)				
	ITERATION NO.				
1 (Pot. Flow)	2	3	4	5	
1	1.000	0.847	0.760	0.816	0.705
2	1.000	0.643	0.683	0.672	0.672
3	1.000	0.891	0.770	0.792	0.782
4	1.000	0.934	0.945	0.863	0.874
5	1.000	0.979	0.979	0.979	0.957

Inspection of the above tables reveals that the solution had converged rather well except, perhaps, at the last spanwise section. However, it should be noted that the tabulated separation locations (predicted by the boundary layer analysis) were modified in the potential flow program in such a way that they are shifted to the trailing edge of the nearest panel close to these locations. This shift in the separation locations may introduce substantial errors, especially if the separation is in the region where panel spacing is sparse. This restriction will be removed during the next phase of development which will have provision to incorporate an arbitrary separation line into the program.

This case is presented here simply to validate the iterative scheme and the computer program. Unfortunately no reliable wind tunnel test data are available at high angles of attack, and hence the computed results are not compared with experiment. At the present time, NASA Langley has been conducting some additional tests on this particular wing in which detailed wake flow measurements are being taken. This detailed information will be very useful during the next phase of the development for the validation of the program.

## 6. CONCLUSIONS AND FUTURE WORK

### 6.1 Conclusions

The development of a basic three-dimensional CLMAX iterative scheme involving boundary layer, potential flow, and separation flow modeling is complete, and the program has been validated by comparing the results with wind tunnel test data for some simple cases. The basic singularity model is represented by panels which are assumed to have linearly varying and constant vorticity along the chordwise and spanwise directions, respectively. This basic singularity model restricts the free vortex sheet deformation to vertical movements only, and hence cannot be applied to close-approach problems in which roll-up must be taken into account. Additionally, the separation locations, predicted by the boundary layer analysis at each of the selected spanwise sections, are shifted to the trailing edge of the nearest panel on the upper surface of the airfoil. In spite of these simplifying assumptions, the major purposes of the present investigation have been accomplished; viz., the demonstration of the feasibility of extending the two-dimensional CLMAX model to three-dimensional flows and the validation of the developed computer program.

### 6.2 Phase II: Leading-Edge Separation and Close-Approach Model

One of the major problems of predicting the vortex surface non-linear interaction using panel methods is the "close-approach" situation. Panel methods have distortions in the velocity distribution close to the panel edges and the problem is present in varying degrees of severity in all panel methods, including the present higher-order method. The three-dimensional form of the close-approach model developed by AMI under a NASA-Ames contract employs a subpaneling scheme based on distributed doublet and source singularities.

The work in Phase II will be based on the new close-approach model. The doublet/source singularities of this model will replace the vortex sheet panels in the basic program of the current Phase (Phase I). The same corner point definition will be used, so the modification should be straightforward.

The restriction of vertical deformation of the shed vortex sheets is not necessary with the close-approach method. Full roll-up of the sheets will be incorporated--in this case a streamline calculation routine will indicate lines of linear doublet intensity (i.e., constant vorticity) on the free sheets.

Procedures will be investigated to allow arbitrary separation lines and to include leading-edge vortex shedding.

## 7. REFERENCES

1. Henderson, W.P., "Effects of Wing Leading-Edge Radius and Reynolds Number on Longitudinal Aerodynamic Characteristics of Highly Swept Wing-Body Configurations at Subsonic Speeds", NASA TN D-8361, December 1976.
2. Polhamus, E.C., "A Concept of the Vortex Lift of Sharp-Edge Delta Wings Based on a Leading-Edge-Suction Analogy", NASA TN D-3767, 1966.
3. Maskew, B. and Dvorak, F.A., "Investigation of a Separation Model for the Prediction of  $C_{l_{max}}$ ", J. of Am. Hel. Soc., Vol. 23, No. 2, April 1978.
4. Maskew, B., "A Submerged Singularity Method for Calculating Potential Flow Velocities at Arbitrary Near-Field Points", NASA TM X-73, 115, March 1976.
5. Maskew, B. and Woodward, F.A., "Symmetrical Singularity Model for Lifting Potential Flow Analysis", J. Aircraft, Vol. 13, No. 9, September 1976, pp. 733-734.
6. Cumpsty, N.A. and Head, M.R., "The Calculation of Three-Dimensional Turbulent Boundary Layers, Part II: Attachment Line Flow on an Infinite Swept Wing", Aero. Quart., Vol. XVIII, May 1967.
7. Bradshaw, P., "Calculation of Three-Dimensional Turbulent Boundary Layers", J. Fluid Mech., Vol. 46, 1971.
8. Cumpsty, N.S., and Head, M.R., "The Calculation of the Three-Dimensional Turbulent Boundary Layers", Aero. Quart., Vol. XX, May 1969.
9. Curle, H., "A Two-Parameter Method for Calculating the Two-Dimensional Incompressible Laminar Boundary Layer", J. R. Aero. Soc., Vol. 71, 1967.
10. Smith, A.M.O., "Transition, Pressure Gradient and Stability Theory", Proceedings of 9th International Congress of Applied Mechanics, Brussels, The Netherlands, Vol. 7, 1957.
11. Granville, P.S., "The Calculation of the Viscous Drag of Bodies of Revolution", David W. Taylor Model Basin Report 849, 1953.
12. Cumpsty, N.A. and Head, M.R., "The Calculation of Three-Dimensional Turbulent Boundary Layers, Part I: Flow Over the Rear of an Infinite Swept Wing", Aero. Quart., Vol. XVIII, February 1967.
13. Gaster, M., "The Structure and Behavior of Laminar Separation Bubbles", ARC 28-226, 1967.

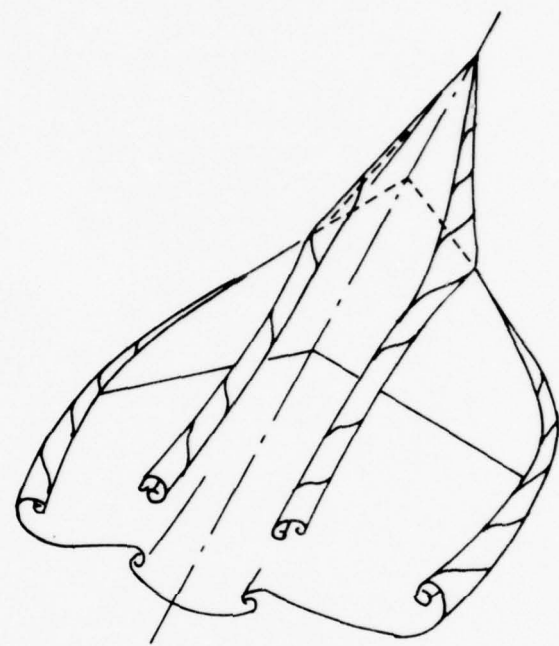


Figure 1. Vortex Flows on a Fighter Wing Planform.

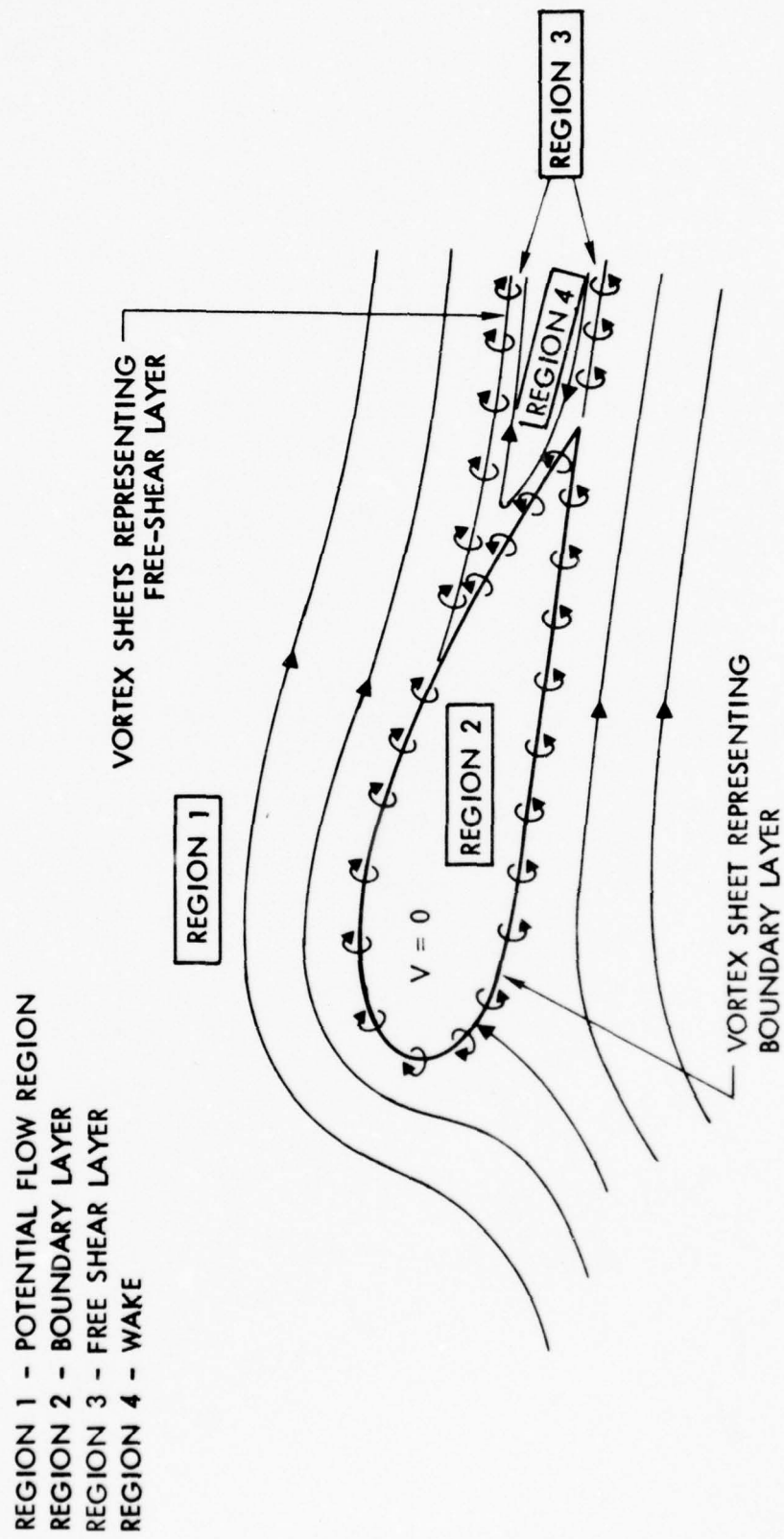


Figure 2. Simplified Vortex Sheet Model of the Separated Flow.

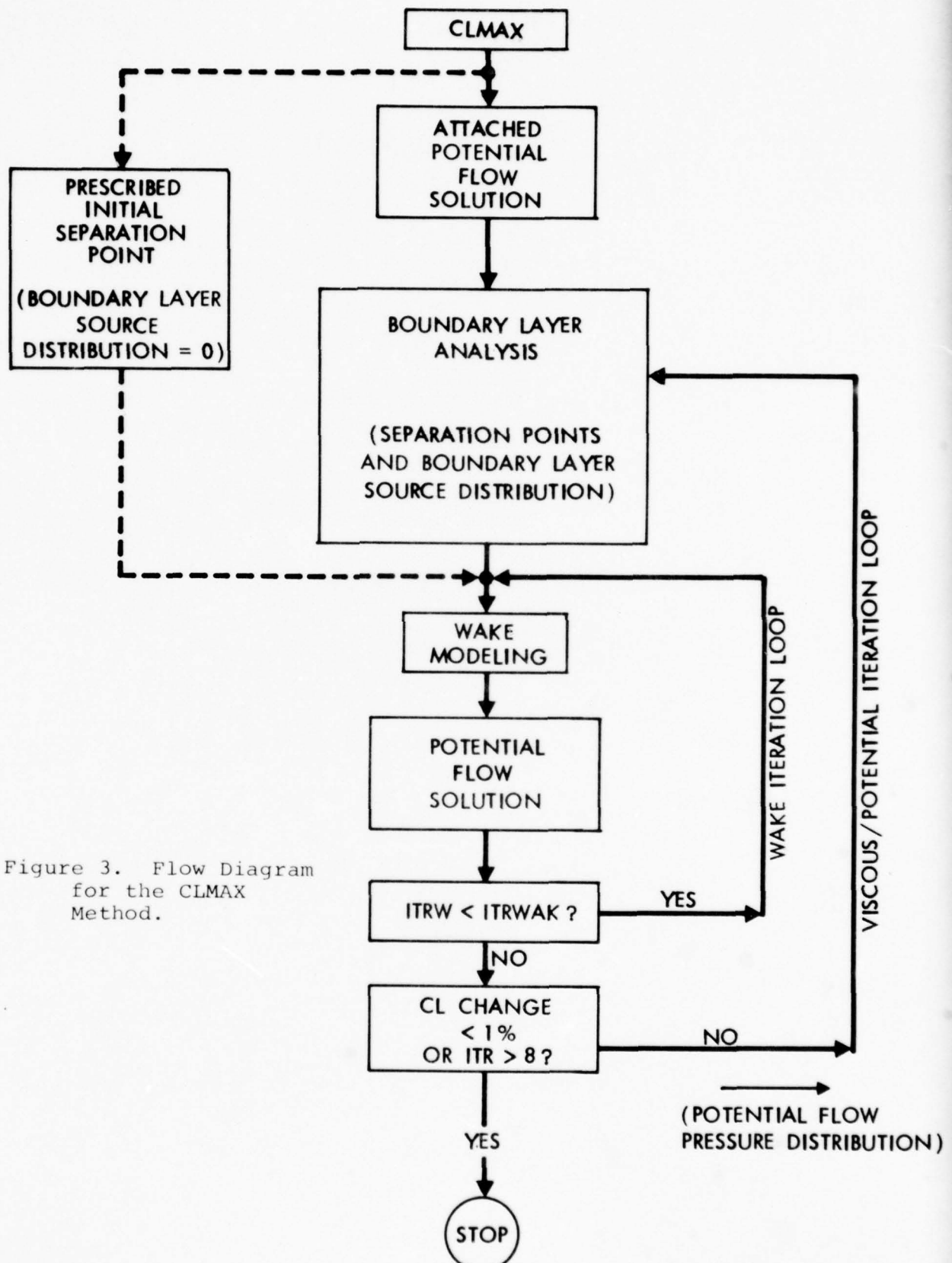


Figure 3. Flow Diagram for the CLMAX Method.

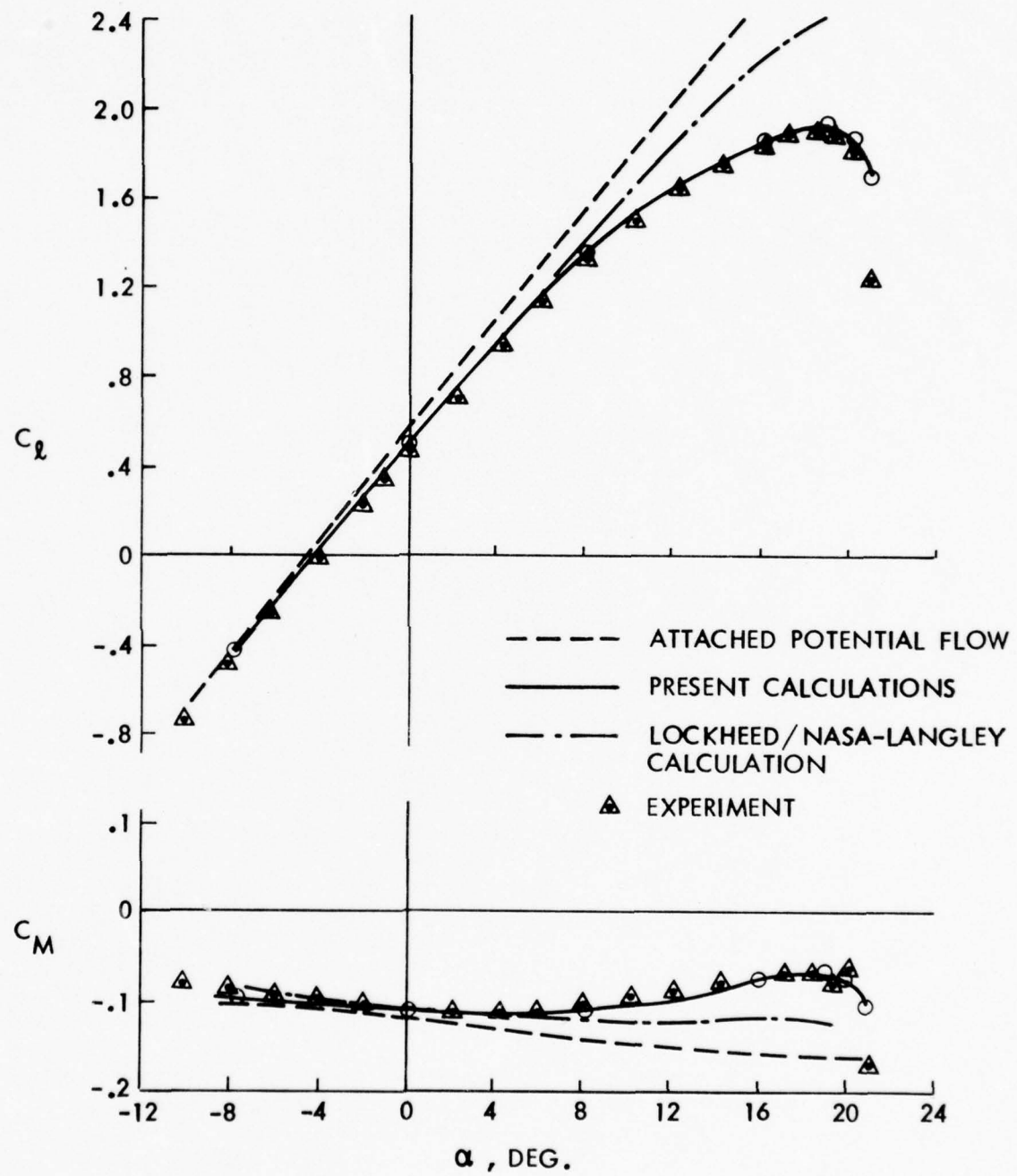


Figure 4. Lift and Pitching Moment Characteristics for the GA(W)-1 Airfoil. Reynolds Number = 6.3 Million.

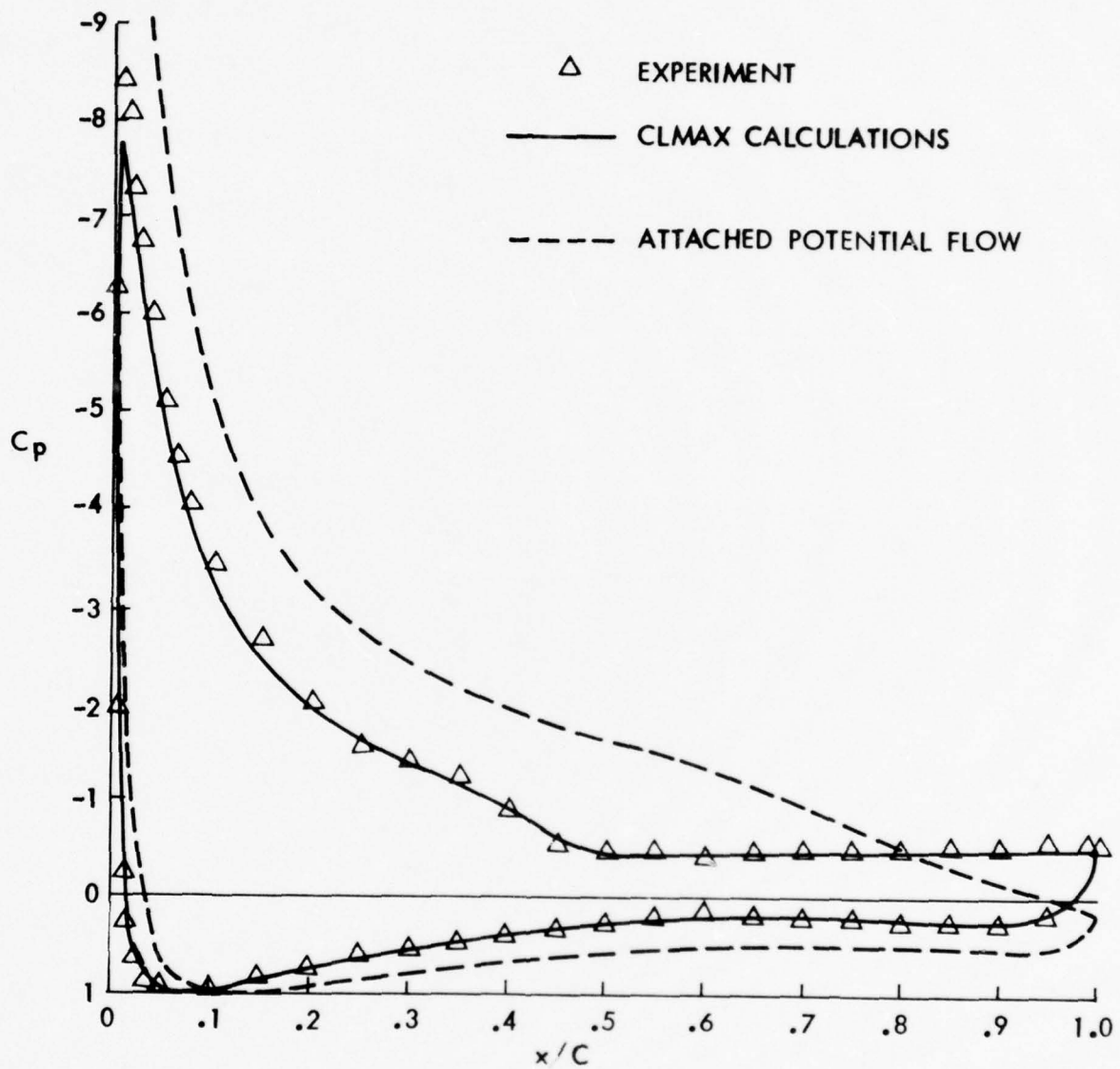


Figure 5. Comparison of Calculated and Experimental Pressure Distribution for the GA(W)-1 Airfoil at  $20.05^{\circ}$  Incidence. Reynolds Number = 6.3 Million.

NACA 4412

○ PRESSURE DATA

□ FORCE DATA

— CLMAX

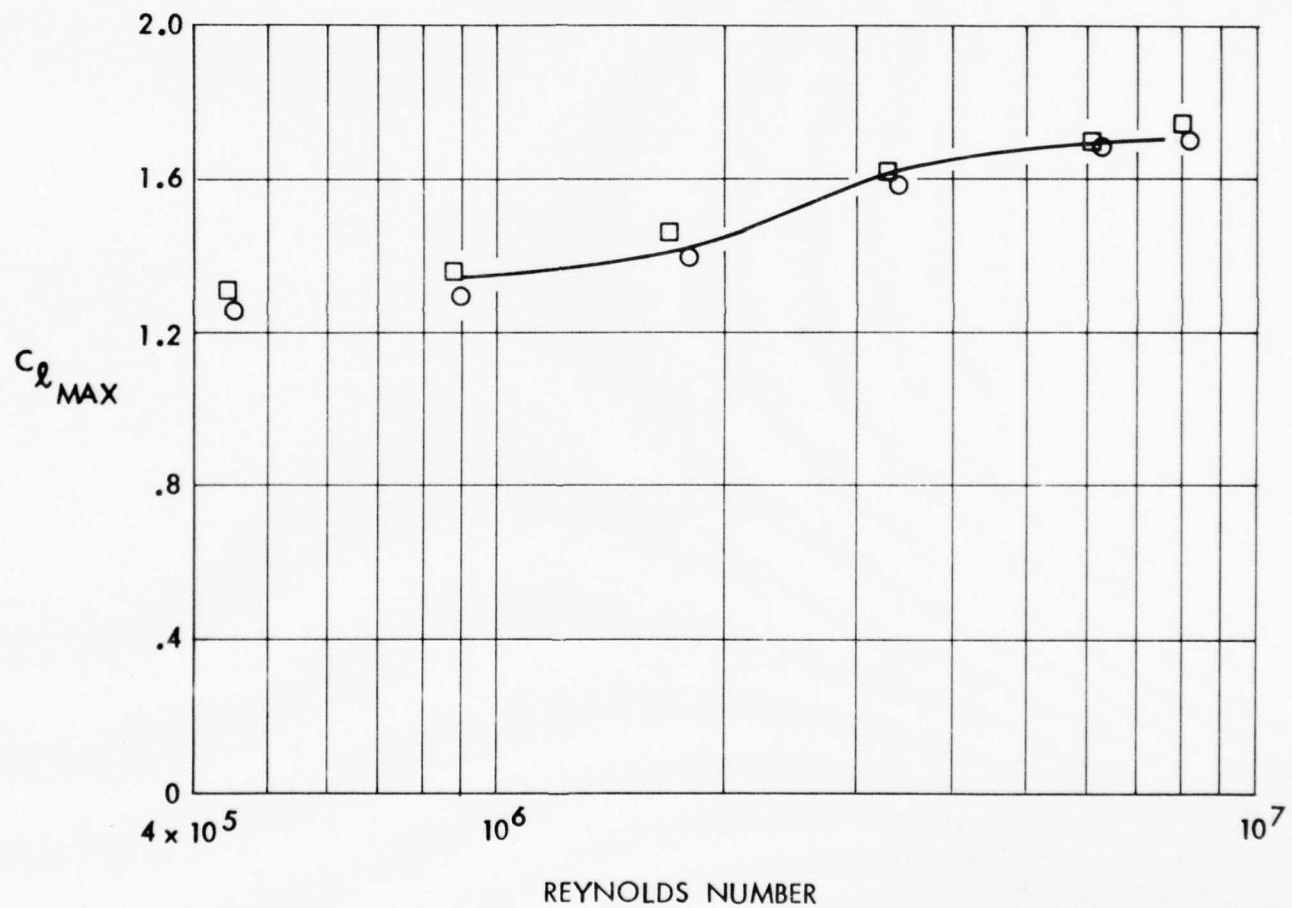


Figure 6. Comparison of Calculated and Experimental Variations of  $C_{l_{\max}}$  with Reynolds Number for the NACA 4412 Airfoil.

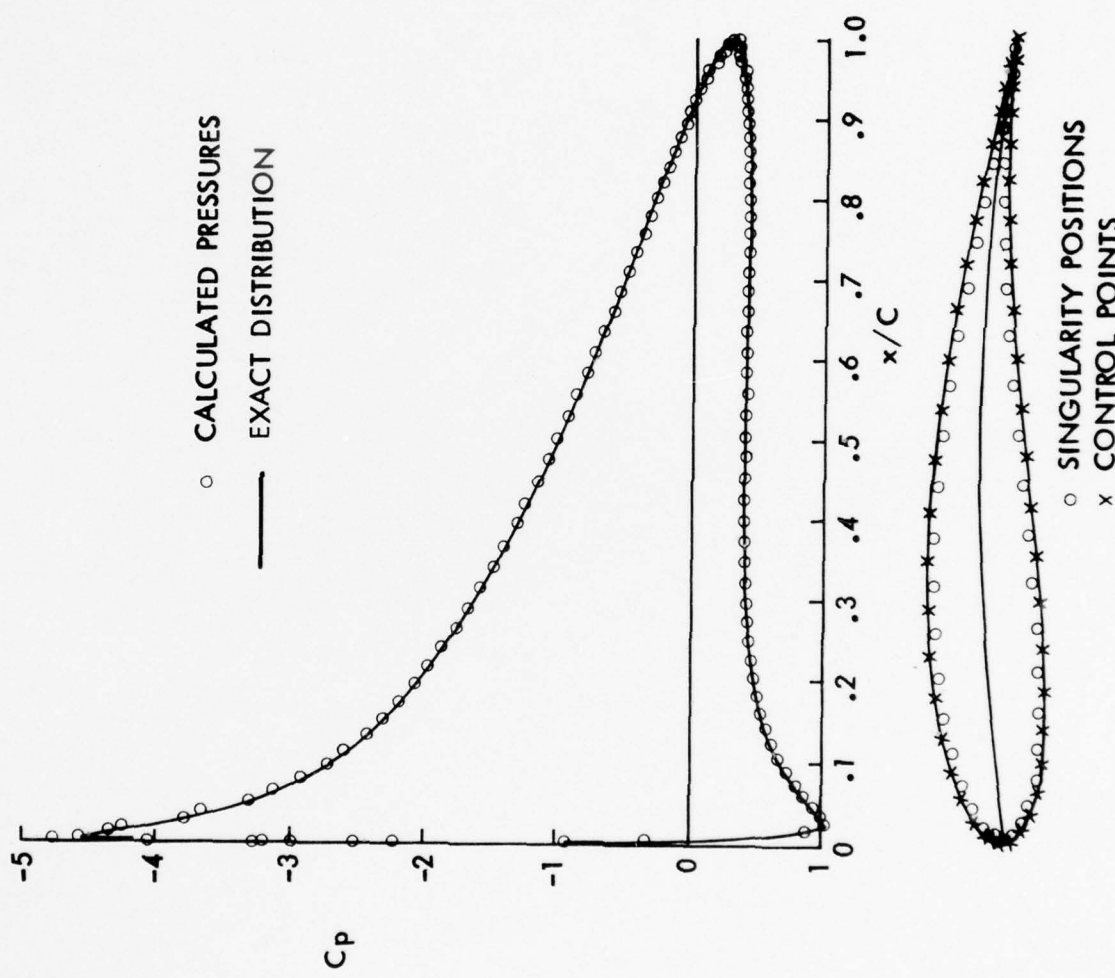


Figure 7. Pressures Calculated at Arbitrary Points on a Joukowski Airfoil at  $10^0$  Incidence. Model: Submerged Vortices and Sources (Coincident) with a Subvortex Technique Applied.

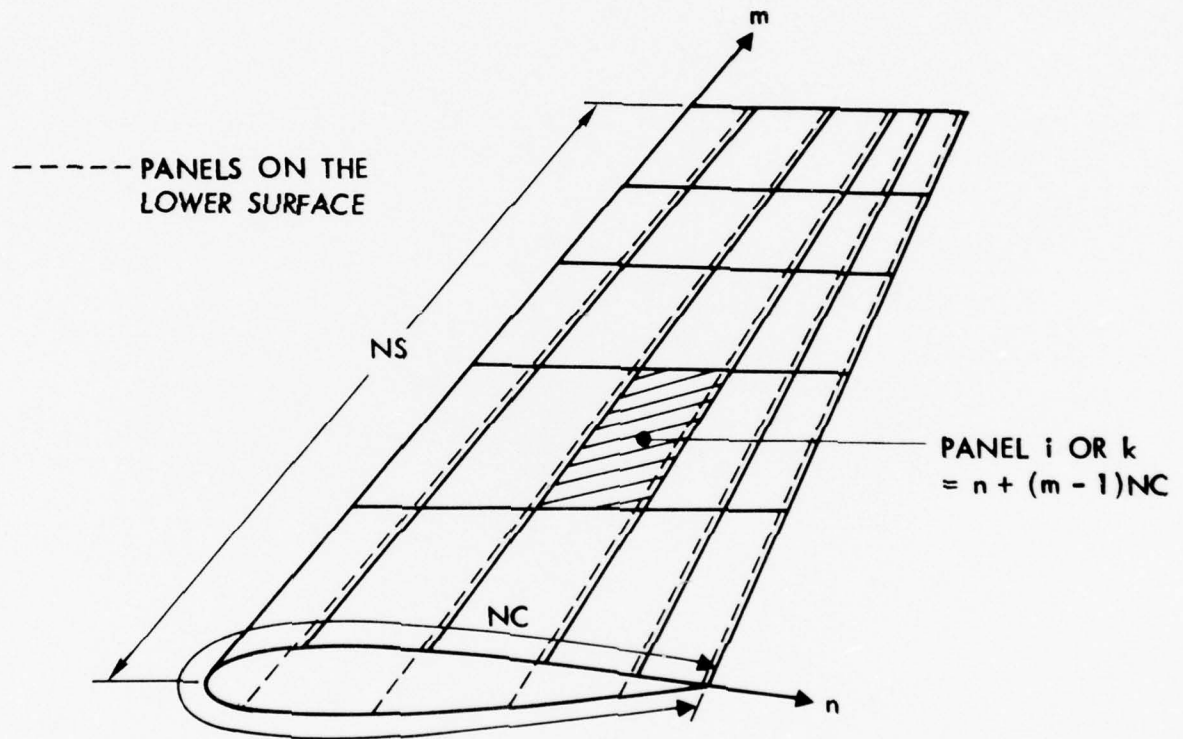


Figure 8. Arrangement of the Panels on a Wing.

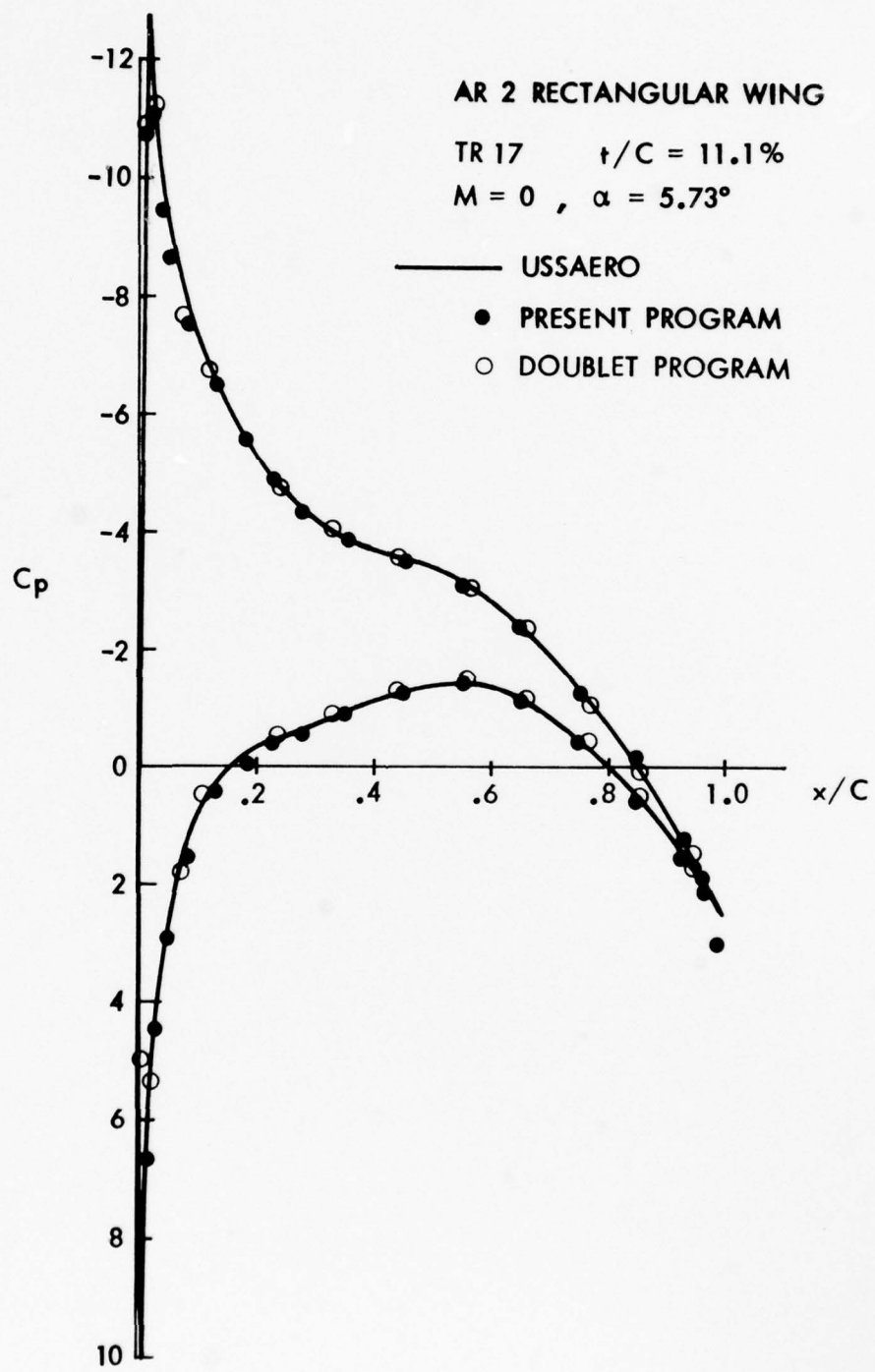


Figure 9 (a). Chordwise Pressure Distribution  
 $(y/b = 0.125)$ .

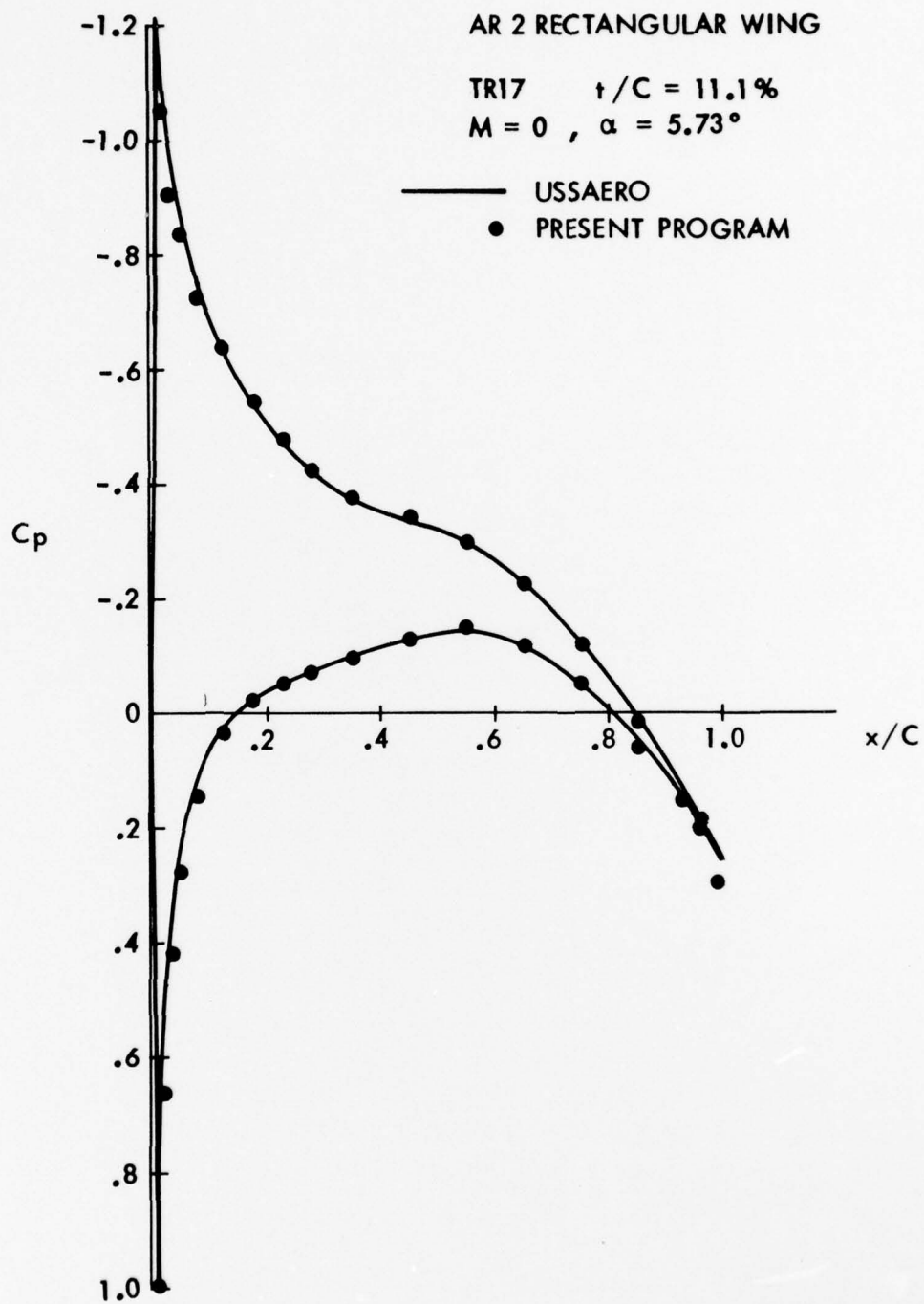


Figure 9 (b). Chordwise Pressure Distribution  
 $(y/b = 0.375)$ .

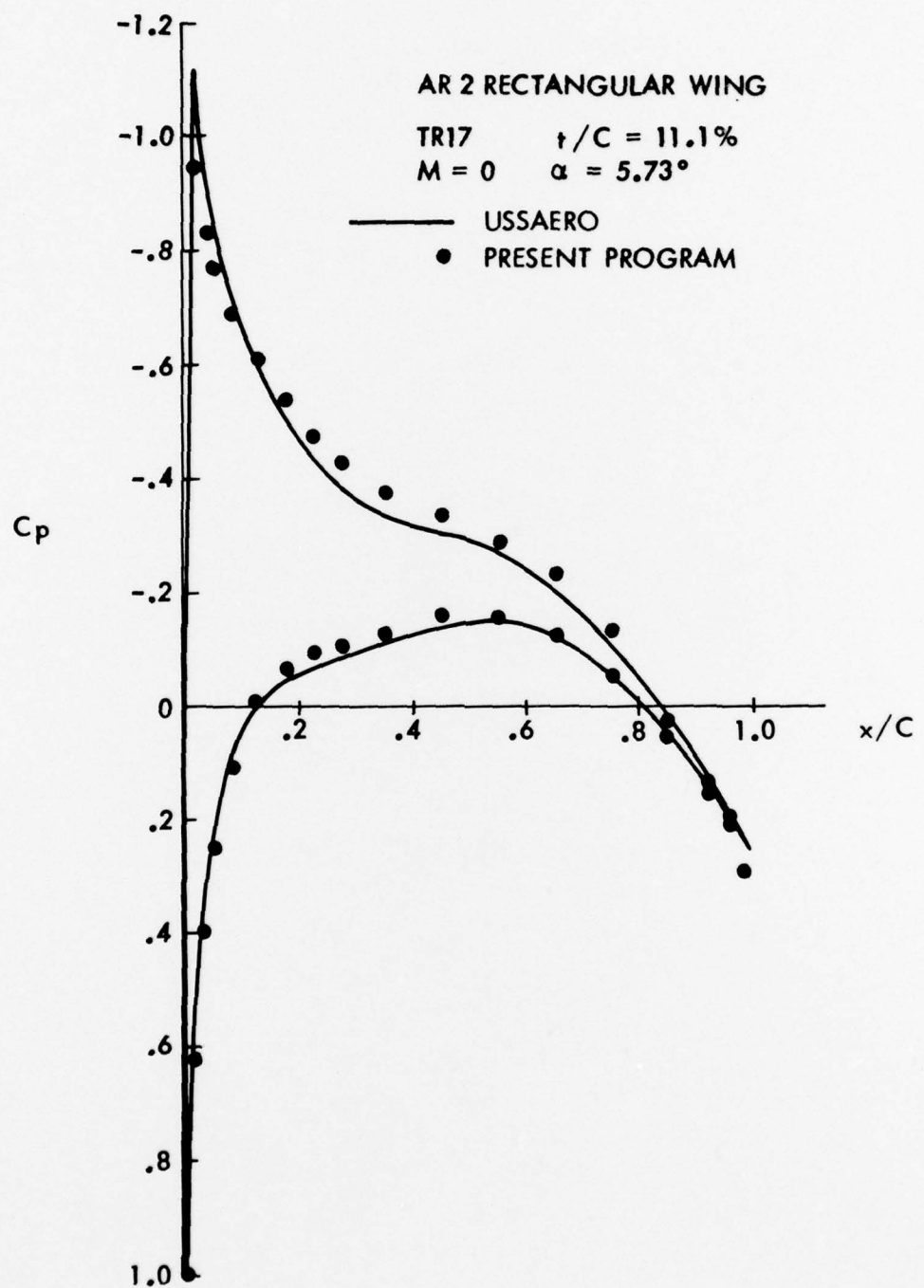


Figure 9(c). Chordwise Pressure Distribution  
 $(y/b = 0.625)$ .

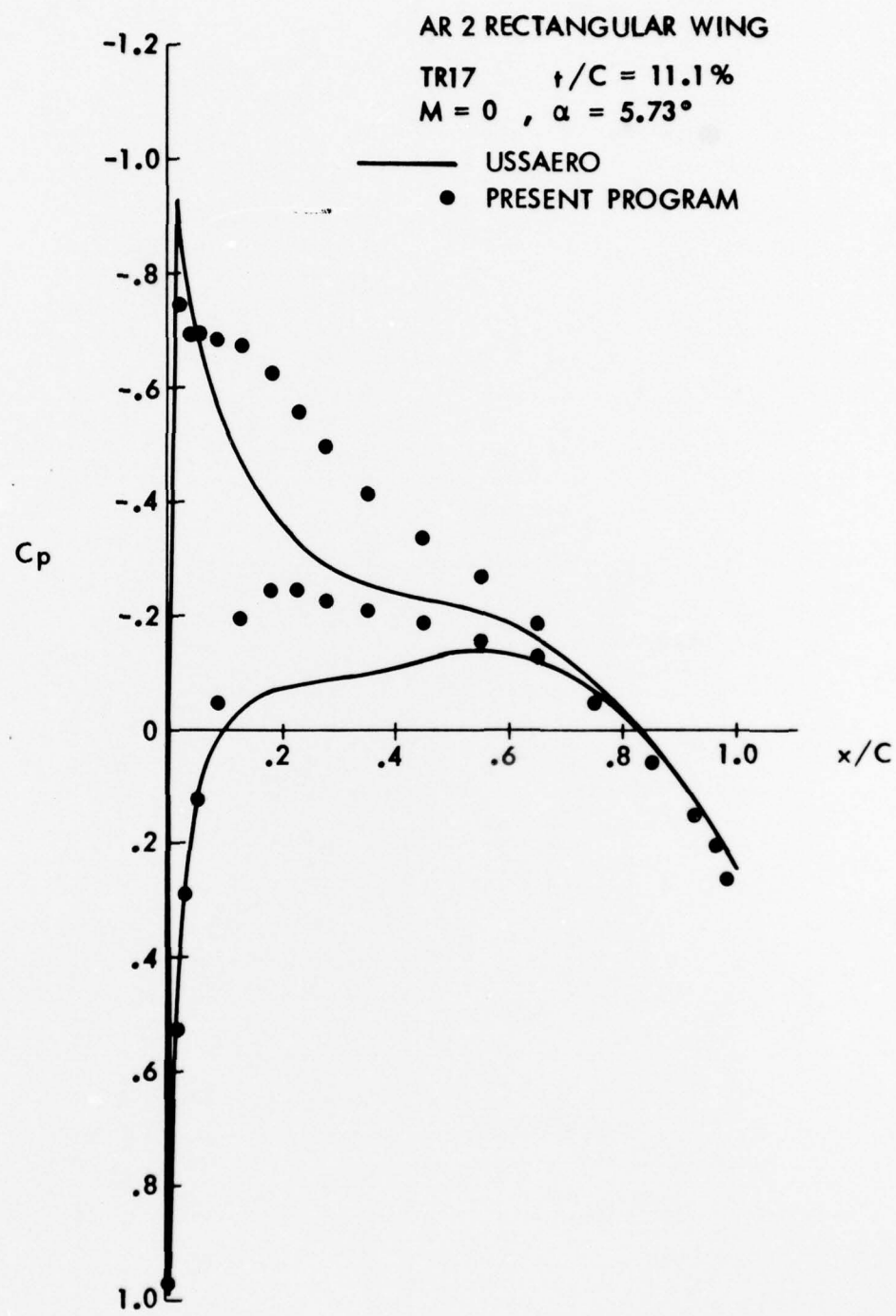


Figure 9(d). Chordwise Pressure Distribution  
( $y/b = 0.875$ ).

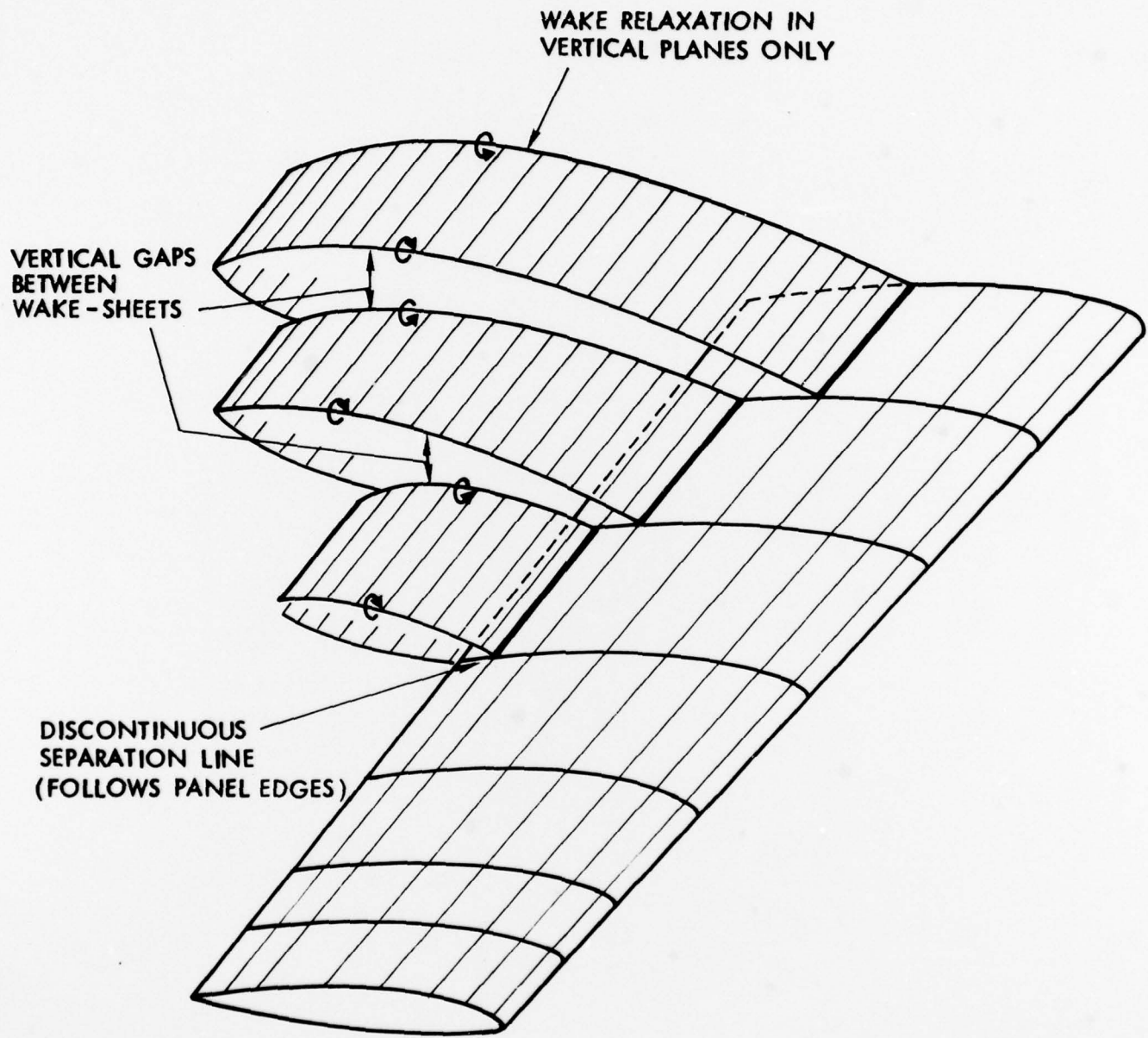


Figure 10. Basic Separation Flow Model.

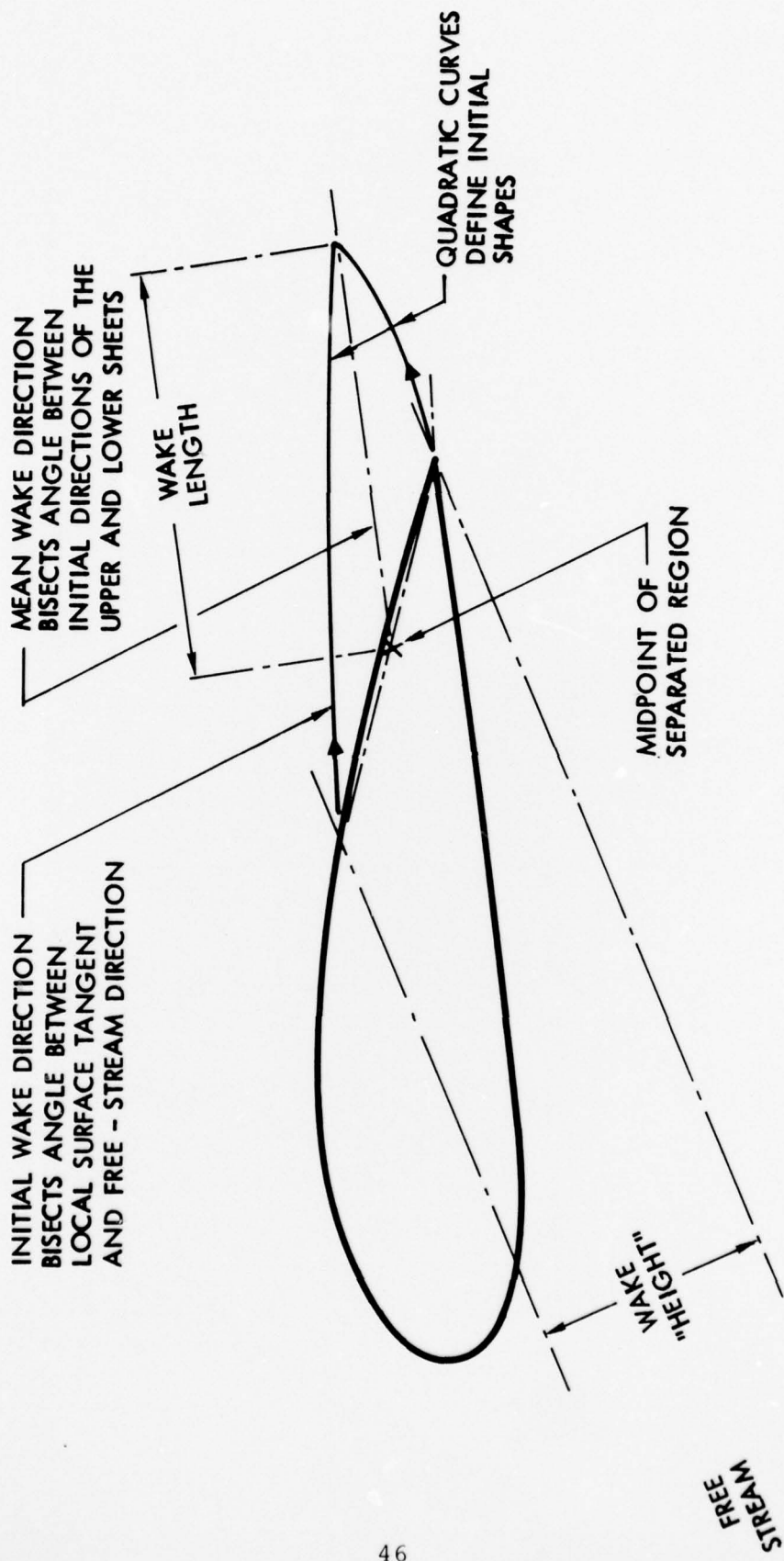


Figure 11. Initial wake Geometry.

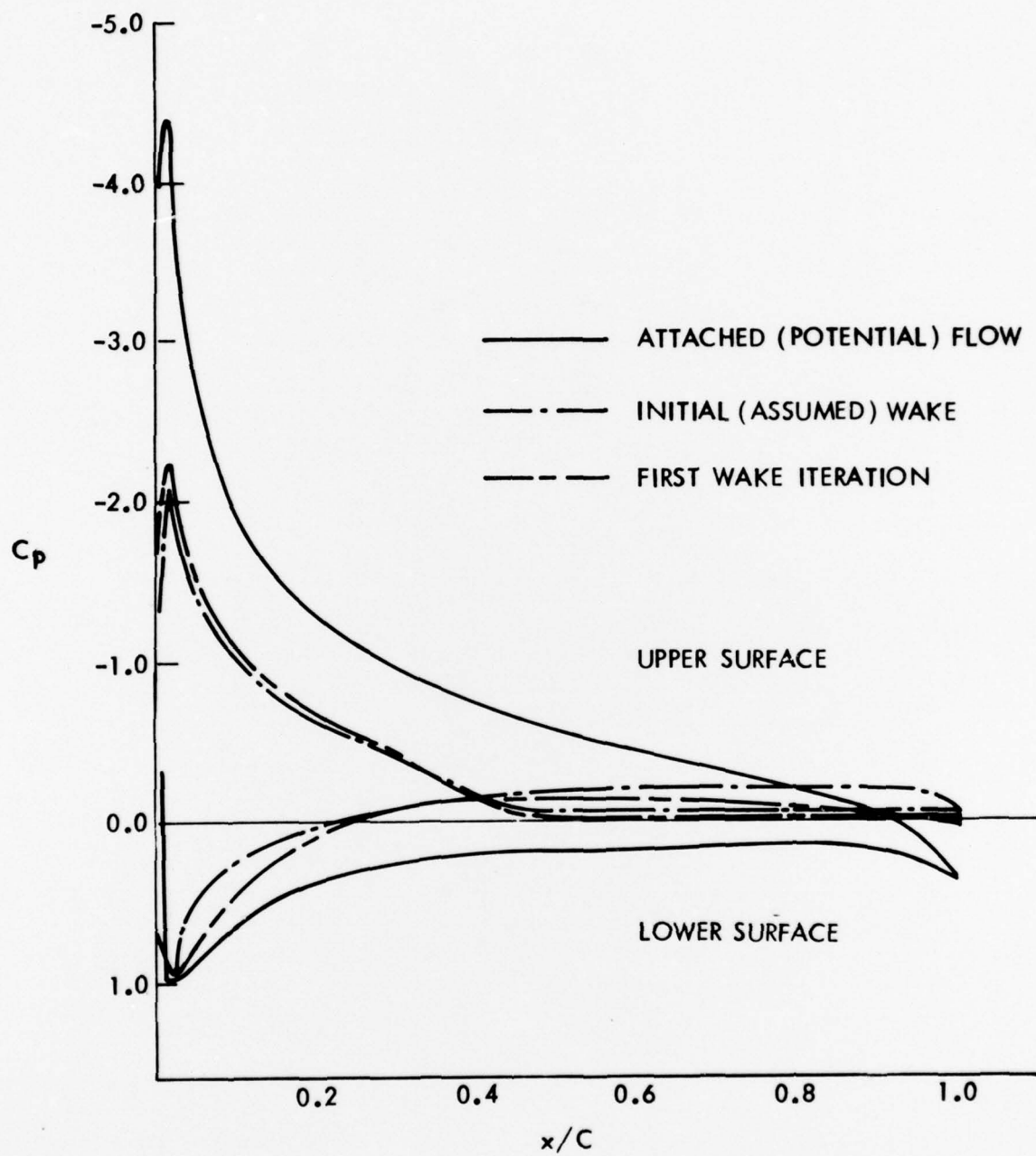


Figure 12. Chordwise Pressure Distribution (Inboard Section).

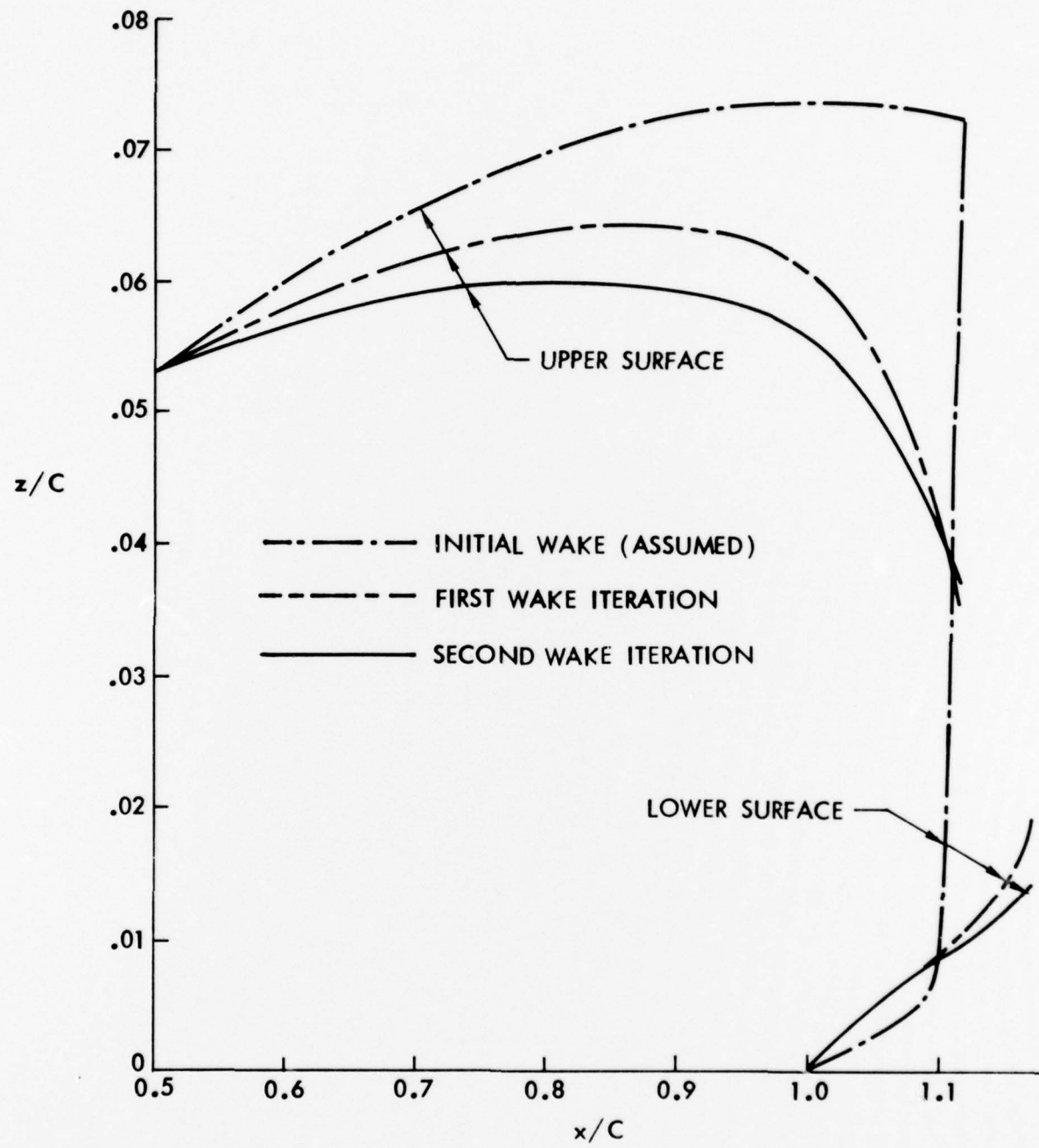


Figure 13. Iterated Wake Shapes (Inboard Section).

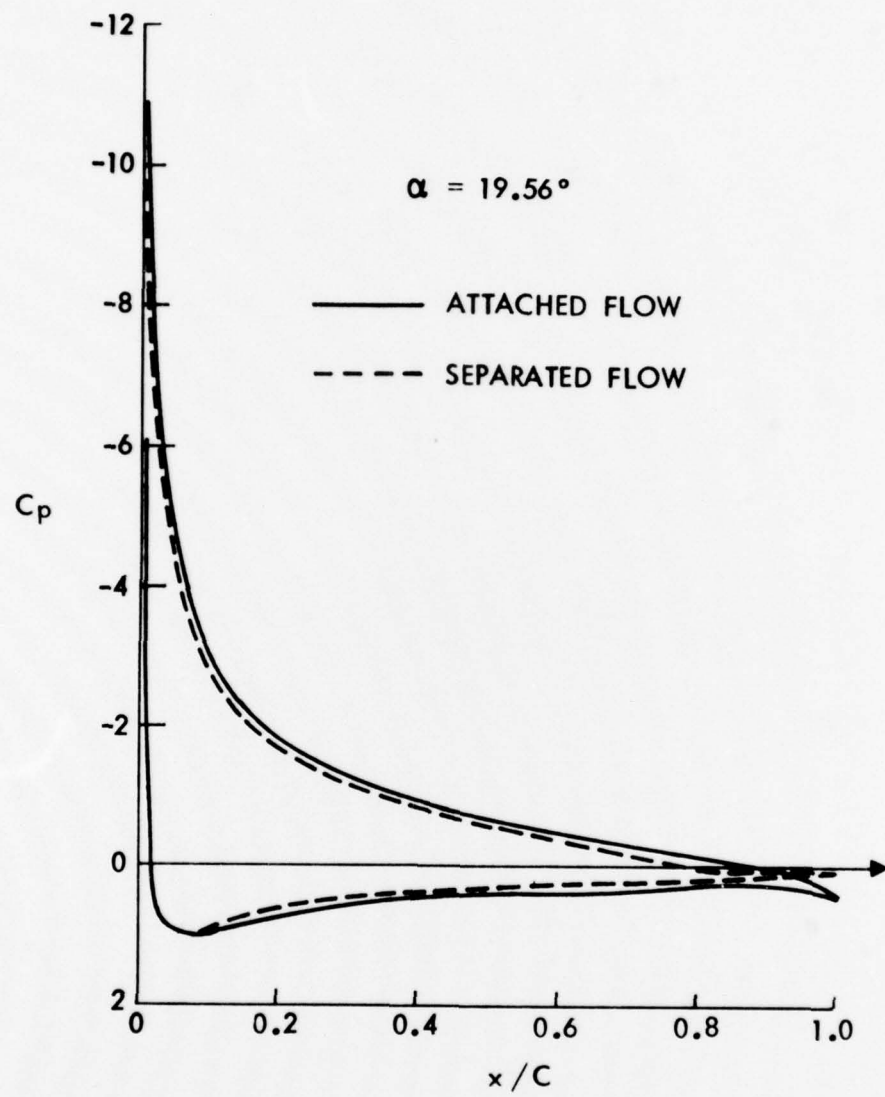


Figure 14. Chordwise Pressure Distribution  
( $y/b = 0.198$ ).

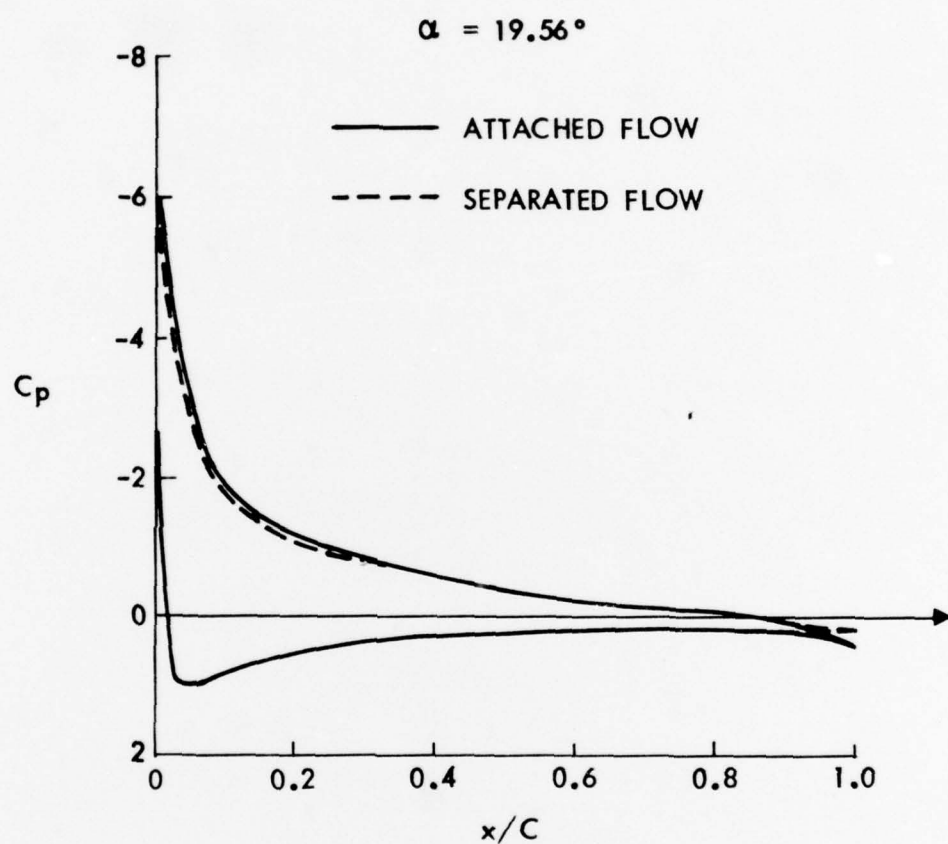


Figure 15. Chordwise Pressure Distribution  
( $y/b = 0.897$ ).

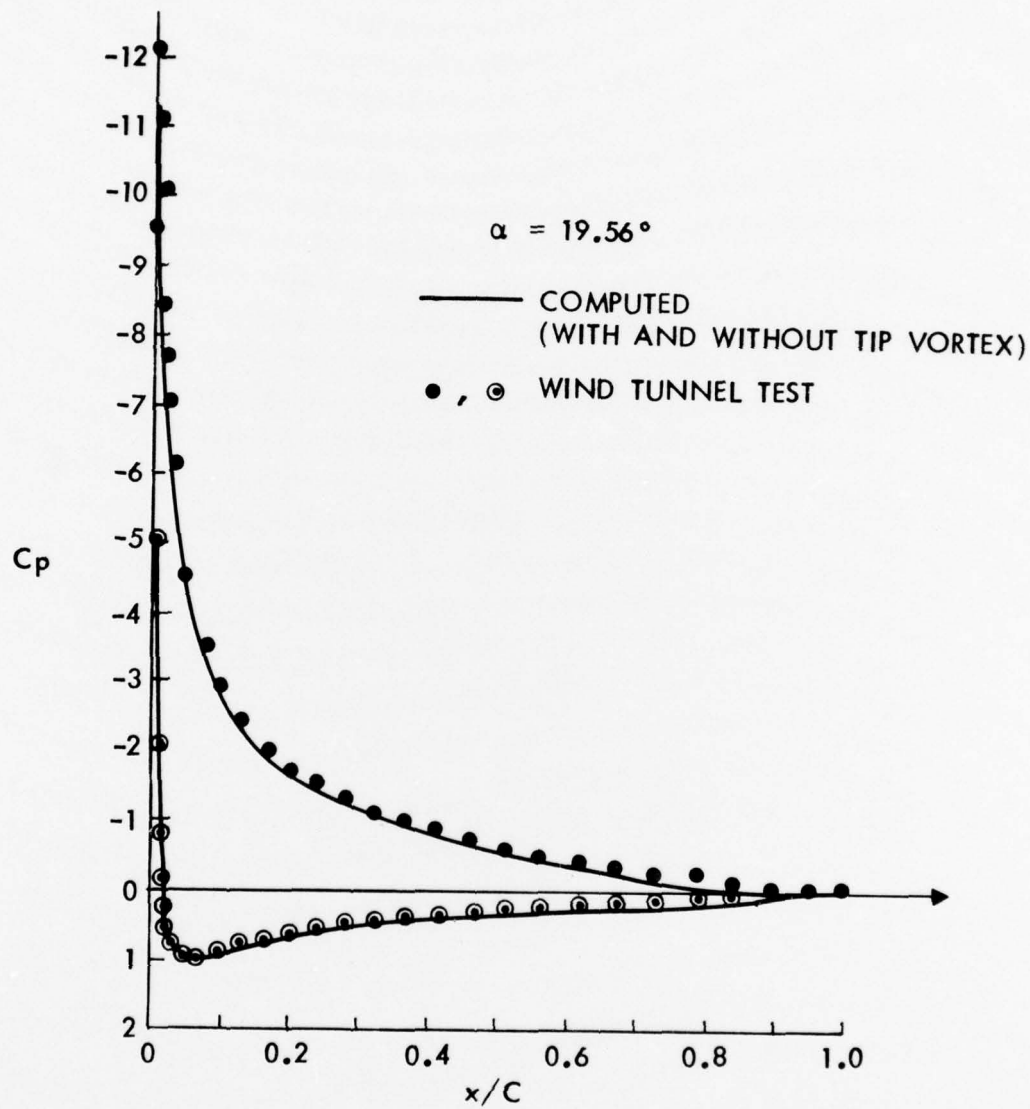


Figure 16. Chordwise Pressure Distribution  
 (Strip 1;  $y/b = 0.18$ ).

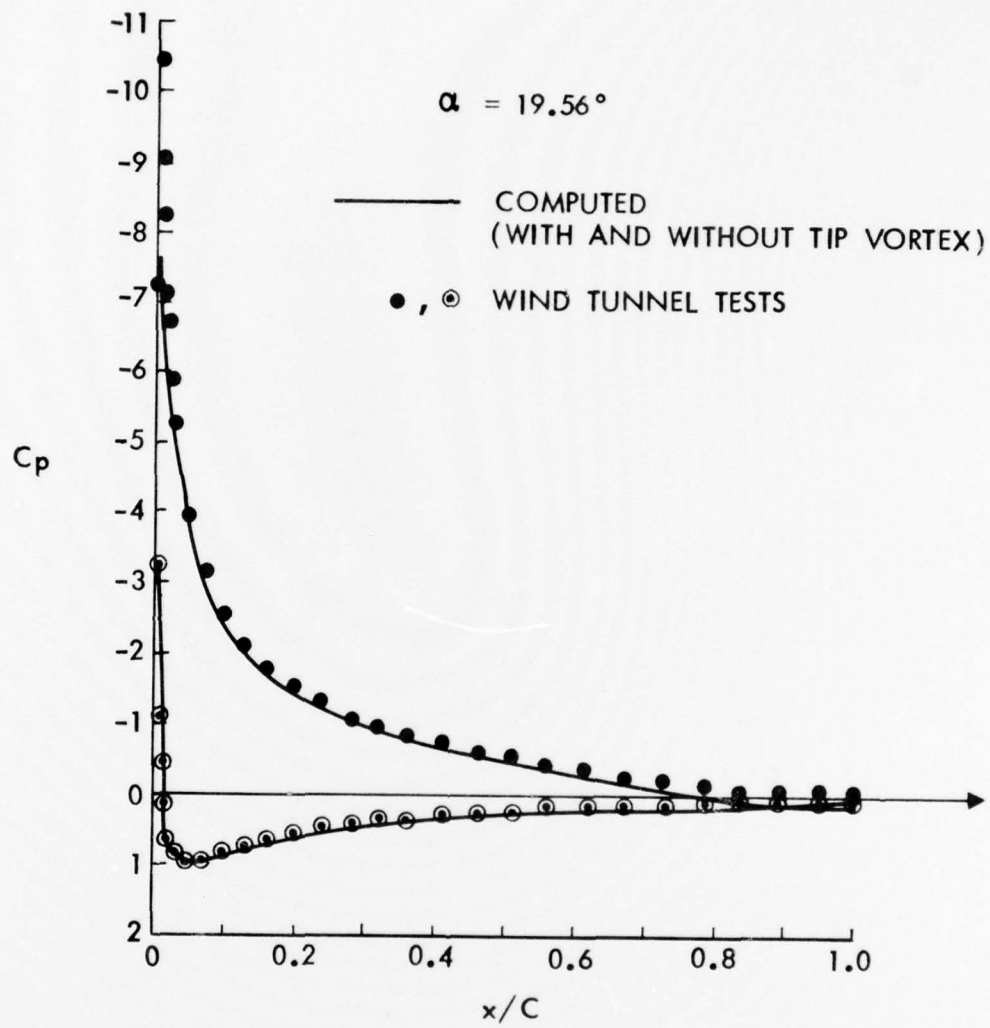


Figure 17. Chordwise Pressure Distribution  
 (Strip 3;  $y/b = 0.695$ ).

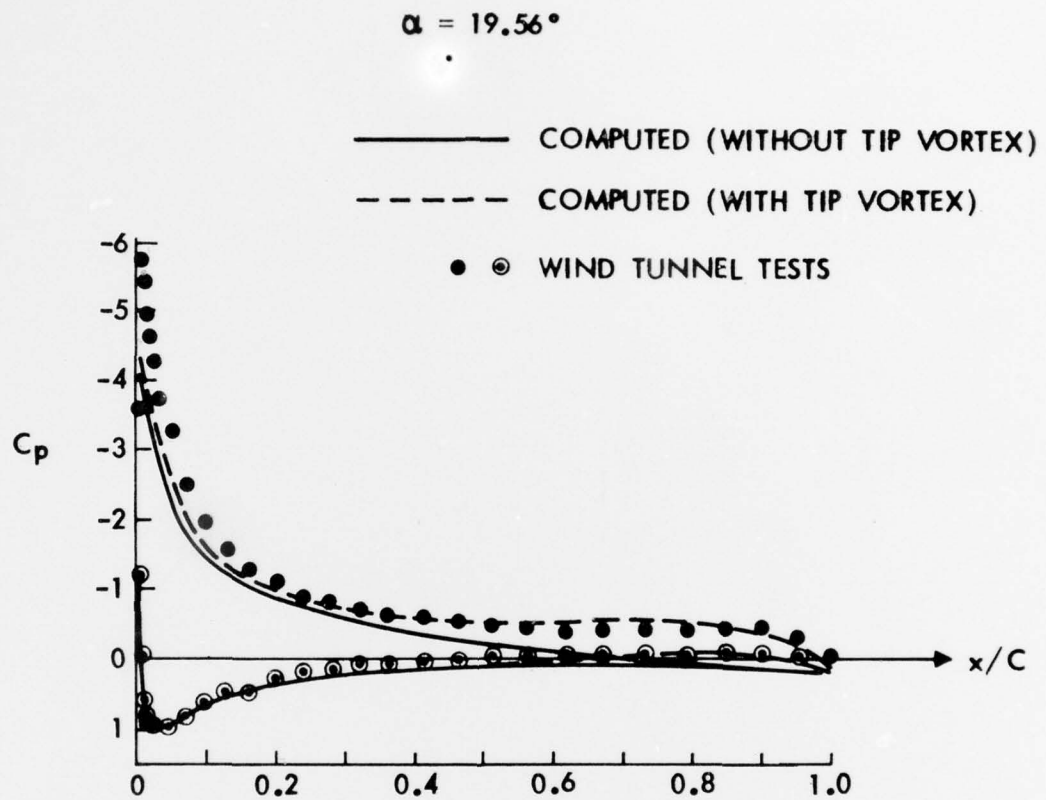


Figure 18. Chordwise Pressure Distribution  
 (Strip 5;  $y/b = 0.95$ ).

DISTRIBUTION LIST

Office of Naval Research 800 N. Quincy St. Arlington, VA 22217 ONR 211 ONR 430C	4	U. S. Naval Postgraduate School Monterey, CA 93940 Dept. of Aeronautics (Code 57) Library	1
Office of Naval Research Branch Office 1030 E. Green St. Pasadena, CA 91106	1	Superintendent U. S. Naval Academy Annapolis, MD 21402	1
Office of Naval Research Branch Office Bldg. 114 Section D 666 Summer St. Boston, MA 02210	1	Air Force Office of Scientific Research Bolling AFB, DC 20332 Code NA (Dr. J. Wilson)	1
Office of Naval Research Branch Office 536 South Clark St. Chicago, IL 60605	1	Air Force Flight Dynamics Laboratory Wright Patterson AFB, OH 45433 AFFDL/FXM (Mr. R. Jeffries) AFFDL/FGC (Mr. Henry Woodard)	1
Naval Research Laboratory Washington, DC 20375 Code 2627 Code 2629	1	Defense Advanced Research Projects Agency 1400 Wilson Boulevard Arlington, VA 22209 Mr. R. Moore	1
Defense Documentation Center Bldg. 5 Cameron Station Alexandria, VA 22314	12	NASA Langley Research Center Hampton, VA 23365 MS 286 (Mr. R. Margasson) MS 287 (Dr. J. F. Campbell) MS 343 (Mr. J. Bowman) MS 355 (Mr. J. Chambers) MS 355 (Mr. W. Gilbert) MS 355 (Mr. E. Anglin)	1 1 1 1 1 1
Naval Air Systems Command Washington, DC 20361 AIR 320D (Mr. R. Siewert)	1	NASA Ames Research Center Moffett Field, CA 94035 MS 227-8 (Mr. G. Chapman) MS 227-8 (Mr. G. Malcolm) MS 227-2 (Mr. D. Bencze)	1 1 1
Naval Air Development Center Warminster, PA 18974 Code 6053 (Dr. K. T. Yen)	2	Lockheed Missiles & Space Co., Inc. Huntsville Research & Engineering Center P. O. Box 1103 Huntsville, AL 35807 Mr. A. Zalay	1 1
David Taylor Naval Ship Research and Development Center Bethesda, MD 20084 Code 16 (Dr. H. Chaplin) Code 522.3 Aero Library Code 1660 (Mr. J. Nichols)	1 1 1		

ENCLOSURE (3)

McDonnell Douglas Aircraft Company P. O. Box 516 St. Louis, MO 63166 Dept. 230 (Mr. R. W. McDonald) Dept. 241 (Mr. R. B. Jenny) (Mr. D. Kotansky)	1	Virginia Polytechnic Institute & State University Engineering Science Dept. Blacksburg, VA 24061 Dr. D. Mook	1
Vought Corporation Advanced Technology Center, Inc. P. O. Box 6144 Dallas, TX 75222 Dr. Gary Hough	1	Sybucon, Inc. 1900 The Exchange, Suite 175 Atlanta, GA 30339 Dr. John Nash	1
Grumman Aerospace Corporation Bethpage, NY 11714 Research Dept. (Dr. R. Melnik)	1	Nielsen Engineering & Research, Inc. 510 Clyde Avenue Mountain View, CA 94043 Dr. S. B. Spangler	1
Rockwell International Columbus Aircraft Division Columbus, OH 43216 Research Dept. (Dr. P. Bevilaqua)	1		
Northrop Corporation Aircraft Division 3901 W. Broadway Hawthorne, CA 90250 Mr. Gordon Hall	1		
Northrop Corporation Ventura Division 1550 Rancho CONEJO Blvd Newport Park, CA 91320 Dr. A. Wortman	1		
General Dynamics Fort Worth Division P. O. Box 748 Fort Worth, TX 76101 Mr. Charles Anderson (Zone 2833)	1		
General Dynamics Convair Division P. O. Box 80847 San Diego, CA 92138 Dr. E. Levinsky	1		
Boeing Aircraft P. O. Box 3707 Seattle, WA 98124 Dr. P. Rubbert	1		

ENCLOSURE (3)